Semi-active shock absorber based on a rotary spool valve

salim kanso

march 2018

ACKNOWLEDGEMENT

This Thesis is the result of several months of collaboration with professors and engineers at LIM(Laboratorio Interdisciplinare di Meccatronica). First of all, I would like to thank God for his never ending grace, mercy, and provision during my life and specially during my studies, I would like to thank my Family for their support and love, I wish to express my sincere appreciation to prof. Tonoli ans Amati and especially eng. Galluzzi for his support and expert advise, at last I would like to thank all my Friends especially Ali alokka and Ashraf khokha.

Introduction

Mechanical design is a complex process, requiring many skills. Extensive relationships need to be subdivided into a series of simple tasks. The complexity of the process requires a sequence in which ideas are introduced and iterated. Design is an iterative process with many interactive phases. Many resources exist to support the designer, including many sources of information and an abundance of computational design tools. Design engineers need not only develop competence in their field but they must also cultivate a strong sense of responsibility and professional work ethic. After the industrial revolution that we have seen since 1920 until these days we have to distinguish in our production. The suspension is probably the single element of a vehicle which mostly affects its entire dynamic behavior. It is not surprising that in the most essential and fun-driving vehicles, suspensions play a central role with an intriguing mixture of technical features and aesthetic appeal. This central role of suspensions in vehicle dynamics is intuitive: they establish the link between the road and the vehicle body, managing not only the vertical dynamics, but also the rotational dynamics (roll, pitch) caused by their synchronized motions. As such, they contribute to create most of the "feeling" of the vehicle, affecting both its safety and driving fun. This thesis has started 2015 by eng. Andrea Vellante supervising by prof. Andrea Tonoli and eng. Renato Galluzzi, the model has built at the Mechatronics Laboratory (Laboratorio Interdisciplinare di Meccatronica, LIM), since then this model has been developing by some students. This thesis has integrated from previous study had been made by engineers and professors as they mentioned up there.

In this thesis we are looking to improve the functionality of the semi active shock absorber based on the rotary valve, by applying some simulation with different software's and at the end apply some experimental tests. In the chapter 1 we introduced the main component of a suspension and function how the suspension act in a vehicle, we specified chapter 2 for suspension classification which also introduce the types a spring and the shock absorber as well, chapter 3 talk about advances classification of suspension systems, in chapter 4 we introduce the the prototype that we are working on and describe the main parts of the model, chapter 5 talk about fluid dynamic analysis of the model using PumpLinx software and how the simulation was applied and illustrate the results, chapter 6 describe the comparison between experimental results that we had and the simulation results, in chapter 7 introduce the functionality of the motor and calculate the the required torque for the spool, in chapter 8 talk about some parts were designed supplement the system and increase the efficiency.

Contents

Chapter 1

Suspensios, Functions, and Main components

1.1 Suspension Systems

To ride comfort is one of the suspension system priorities, it might appear like the suspension framework is just an arrangement of springs and shock absorber which interface the wheels to the vehicle body. A vehicle suspension framework support a comfort over gruff street while guaranteeing that the wheels stay in contact with the ground and vehicle roll is limited. The suspension framework consist of three main component: a structure that backings the vehicle's weight and decides suspension geometry, a spring that transform energy from kinematic form to the potential one, and finally the shock absorber that is a mechanical gadget intended to disseminate kinetic energy. The suspension system support the vehicle by linking the wheels to its chassis, we can notice the relative movement through the wheels and the chassis body,hypothetically , the whole suspension system reduce the A car suspension associates a vehicle's wheels to its body while supporting the vehicle's weight. Hypothetically, a suspension ought to decrease the rear wheel's degree of freedom from six to two dof, and for the front wheels down to three dof. the system must support the breaking , controlling and propulsion. the relative movement of the wheels can control the movement of the vehicle.

1.2 Function Of Suspension Systems

As before specified it is generally known that the main aim of a suspension system is the assimilation the street roughness. The suspension interfaces the vehicle's body to the ground so its absorb all the vibration and all the forces between these two. The designer always study and take in account three main arguments.

• **Ride Comfort** :Ride comfort is characterized in view of how a rider feels inside a moving vehicle, ride quality can be evaluated by the passenger inside a vehicle, if we consider the vehicle as a whole system there are many disturbances and vibration we can refer them into inner disturbances and outer disturbances, giving some examples for inner one like the vibration of the engine and the movement of the transmission, the outer disturbances like the vibration caused from road profile. The comfort vibration would be between this frequency range (0-20 HZ) and not comfortable between (20-20000 HZ) .

• **Road Holding**:Realizing the Forces those act between the wheel and the street, these forces act on the suspension system as well. The road holding support the vehicle specially through controlling , breaking while the vehicle turn.

•**Handling** : We can check the quality of the suspension system and guarantee that the vehicle will be steady in each move and that the good one. But the perfect one is more than checking the stability, the vehicle should react to the riders orders proportionally when there is any change in the steering commands. another task should the suspension do is decrease roll and the pitch movement of a vehicle.

1.3 Main Components Of Suspension Systems

The structure of the suspension is represented in these 4 components: spring, shock absorber, mechanism, bushing s shown in Figure 1.1 on page 7.

•**Mechanism** : The mechanism of the suspension system are the arms connect the vehicle with the wheels and its may have one or more arms depend on the type of the mechanism, the mechanism disturb all the forces in the contact point in all direction between the wheels and the body of the vehicle. It is one of the biggest part in the suspension system it set the geometry which effect the handling and the road holding. The weigh of the mechanism play an important role on the handling, in the automotive structure they prefer the light material which lead to a high efficiency.

• **Spring**: There are many material can be used to fabricate a spring, the most famous shape of the springs take the winding one, we can control the functionality of the spring by controlling the stiffness, the higher stiffness mean the higher road holding and handling but also limit the comfort of the rider, and vise verse. so the most important of designing a spring to choose the appropriate stiffness.

• **Shock absorber**: The bushings is made of rubber used as vibration and noise isolate and it stop the direct contact, there are many types of bushing and

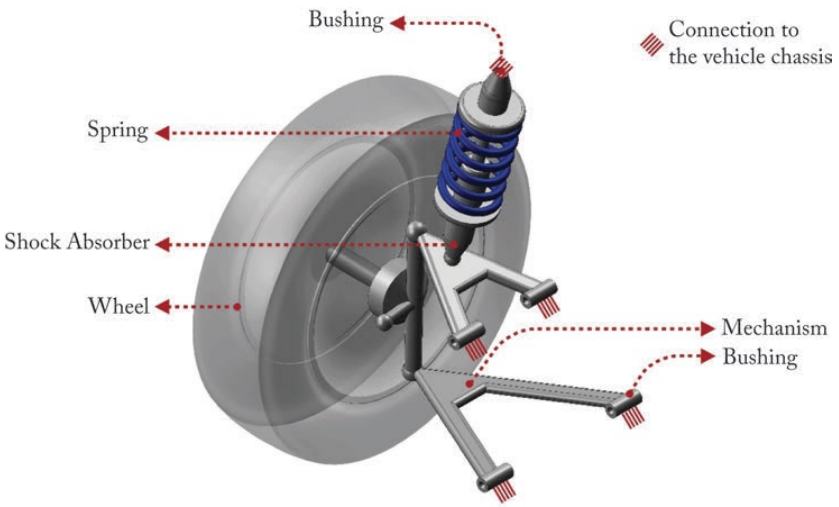

Figure 1.1: The main components of a suspension system[2] .

they labelled depends on their degree of freedom and the most famous one is the re-volute joints, as a matter of fact the bushing is more expensive than the other part in the suspension system.

1.4 Desired Features Of Suspension Systems

These are some requirement we need to check any suspension system.

•**In-dependency** : This is an important properties should the suspension system always have, it represented when a wheel goes through an obstacle and the other wheel is independent from the motion. Giving an example in Figure 1.2 on page 8, the suspension system is independent so we can see a wheel goes through a bump and the wheel doesn't effected. This property can increase the rider comfort and road holding.

• **Good camber control**: The camber angle is the angle of the all wheels about their axis, there is two type of camber angle the positive and the negative angle, the negative camber angle can increase the handling , the negative camber angle tense decrease the wheel endurance, so we can conclude the negative one is more convenient. As you can see (Figure 1.3 and 1.4 on page 9).

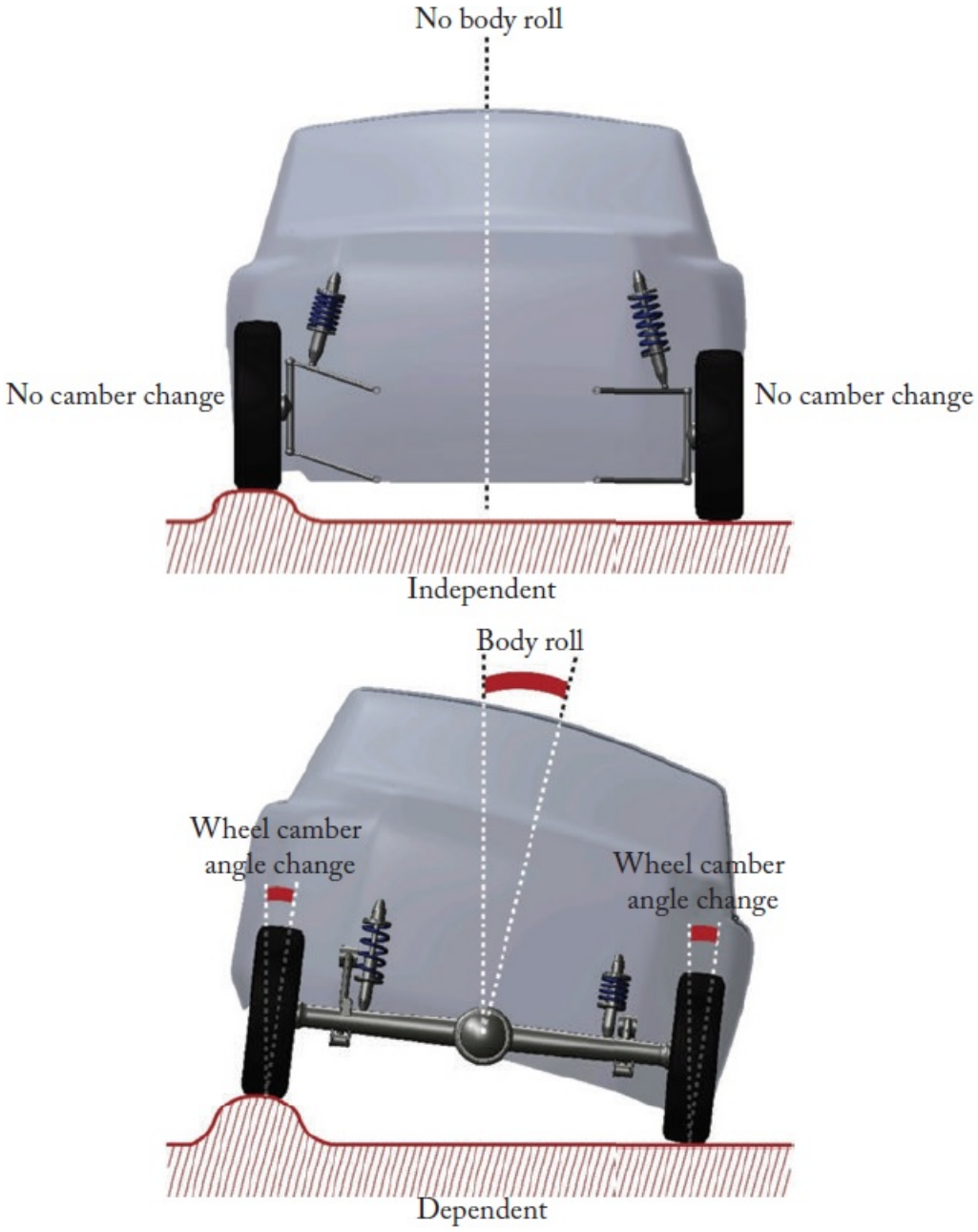

Figure 1.2: Independent vs. dependent suspension systems [2].

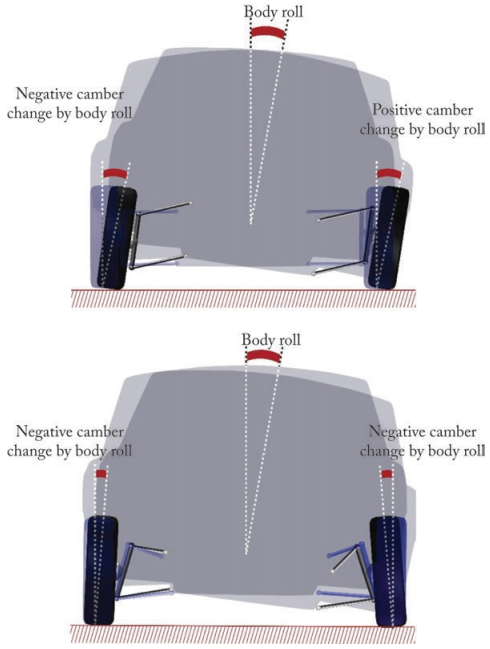

Figure 1.3: Effects of suspension design on camber change due to body roll [2].

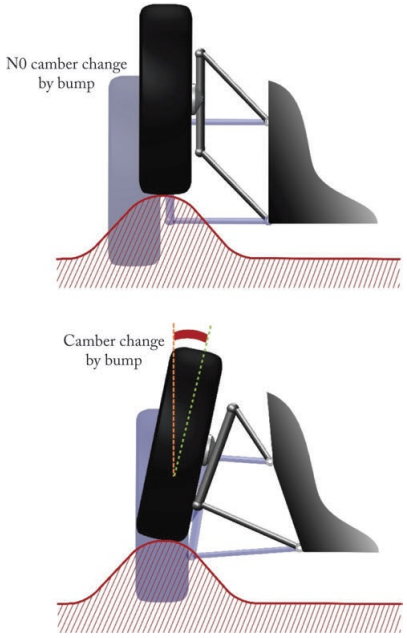

Figure 1.4: Effects of suspension design on camber change due to road bump [2].

• **Good body roll control**: Each suspension system has a roll center. The hypostatical line that connects the front and rear suspensions' roll centers is called the roll axis. The vehicle's body rolls about this line during cornering maneuvers. It is necessary to analyze the roll axis because of its effect on the body roll and lateral vehicle behavior. The design of the suspension geometry should account for the best location of the roll axis in order to optimize vehicle body roll motion.

• **Good isolation**: Enhancing the quality of the suspension systems and isolating the road harshness, this is a very important job job of the suspension system.

• **Good space efficiency**:The design and the shape of the suspension system can effect on over all efficiency, also choosing the type of the suspension determine the required space that we need,the suspension system should drop enough space for other components and should not interface the border of the vehicle (Figure 1.5 on page 10).

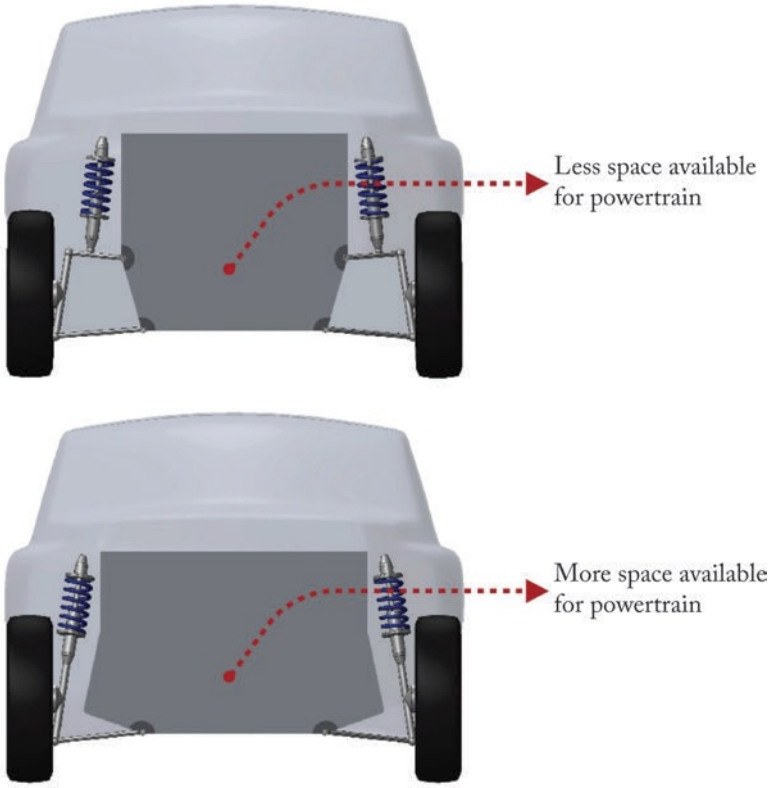

Figure 1.5: Space efficiency of suspension systems [2].

•**Good structural efficiency**: The main function of the suspension system is to handle the vehicle's mass and deal with all the forces those act on the vehicle because the road profile, another job of the suspension system is to distribute the forces through the vehicle body (1.6 on page 11).

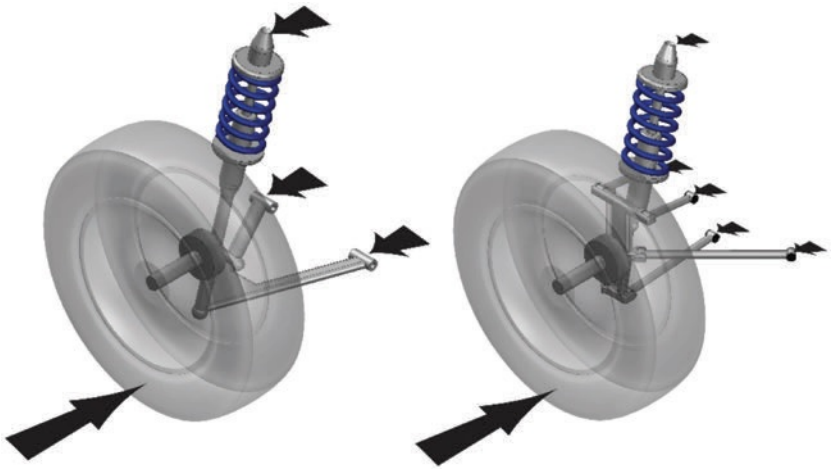

Figure 1.6: Space efficiency of suspension systems [2].

• **Low weight**: There is a obvious relationship between the suspension system and the kinematic energy caused by the suspension system and the overall weight. A high kinematic energy mean higher forces the vehicle would absorb, By choosing the proper and light material for the suspension system would decrease the overall weight and also could increase the design cost, its necessary have a balance between the wight and the cost.

• **Long life**: Long life of any mechanical component is an issue for all designers and specially for the suspension system because it is the most part consumed compared with the others, it also have to be durable more than other component. The quality is proportional to the cost of the suspensions.

•**Low cost** : As we can noticed from the previous requirements, most of them link directly on indirectly to the cost, we should pick up the right suspension for the right vehicle. A high interpretation means a high cost. To increase the quality f the ride a light material should be used, using also a good spring and a good shock absorber also increase the quality, but in other hand increase the cost of the parts.

1.5 Shock Absorber Types

Because our interest about shock absorber we would introduce a little bit the shock absorber and describe also the types of the shock absorber. So the shock absorber is a cylinder that moves inside a closed chamber fulled of oil, it is usually contain one way valve that let the fluid which in this case let the oil pass slowly from one piston to the other. To control the stability and maintain the ride comfort we use a shock absorber. we would describe three types of shock absorber.

1.5.1 Twin Tube

The shape of twin tube shock absorber comprises of two cylinder tubes as shown in Figure 1.7a on page 12. At the base of the internal tube we could realize a valve that enables oil to stream between the tubes. The cylinder goes up and down into the inward tube while the external tube fills in as store. Oil shift between upper chamber and lower chamber of the internal tube through the cylinder valve and also the internal and external tubes through a valve. The damping part in the system is controlled by the orifice valve.

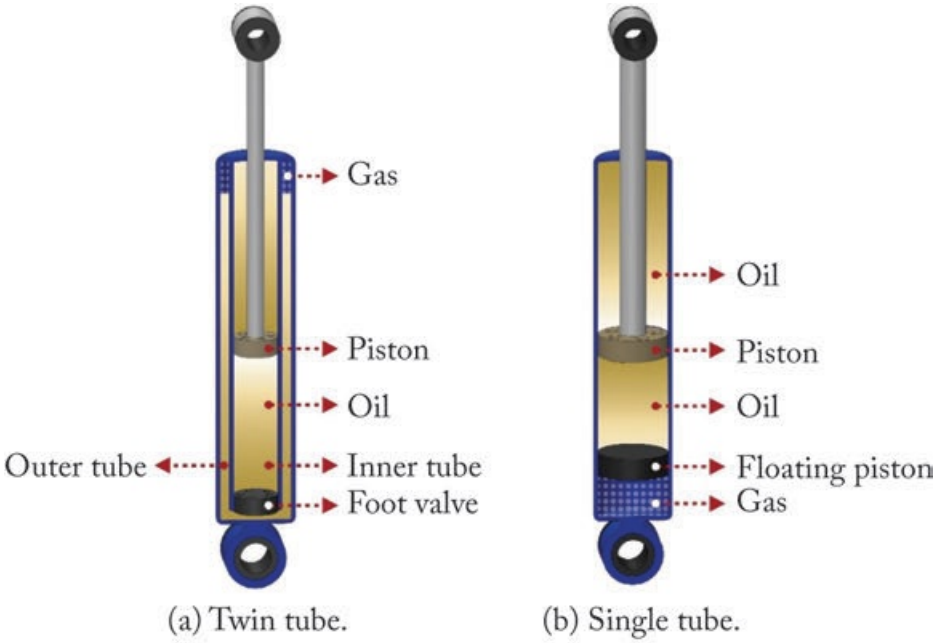

Figure 1.7: Shock absorbers: (a) twin tube and (b) mono tube [2].

1.5.2 Mono Tube

As its name demonstrates, a mono tube shock absorber comprises of one tube that is contain two segments by two cylinders, one is filled by the oil and this the bigger part, the second part is filled with nitrogen gas, these parts separated by a floating piston made of plastic or metal material, preventing them of mixing. As shown in Figure1.7b. When the shock absorber compressed, the rod start moving into chamber and compress the gas chamber, helping the floating piston to move reducing the size of the gas chamber. By disparity when the shock absorber is extended and the rod move out from the working chamber, reducing the volume of the gas chamber which causes it to rebound moving the floating piston again.

1.5.3 Anit-Roll Bar

Anti-Roll Bar is linked the two rear wheels via torsional bar which act as torsional spring As shown in Figure1.8. At the moment the rear wheels on a hub move in a similar war, the anti-roll bar remains inoperative. When the wheel move in inverse way the bar start to torsion and it compelled to twist.

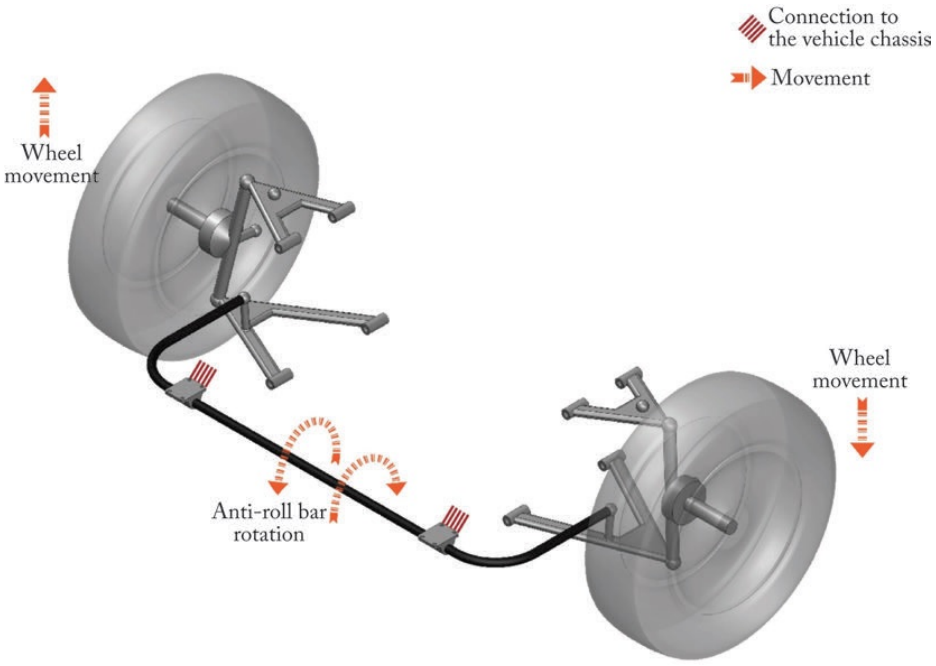

Figure 1.8: Anti-roll bar connects the wheels of an axle to provide torsional stiffness [2].

Chapter 2

The Damper Prototype

A mix of these elements like time-changing parameters , nonlinear behaviour, steady state, asymmetrical control bound, These highlights make the idea of designing a semi-active suspension system very complicated. After all the technologies that we have reached in 20th century, the semi active suspension system it's favourable between all the suspension because the power request is small comparing with others and also control band width. In Politecnico di torino,the Mechatronics research center has begun up taking a shot at (semi-dynamic safeguard in view of a rotational spool valve) venture two or three years back, endeavoring to think about the highlights and enhance the working of the damper as appeared in Figure 2.1.

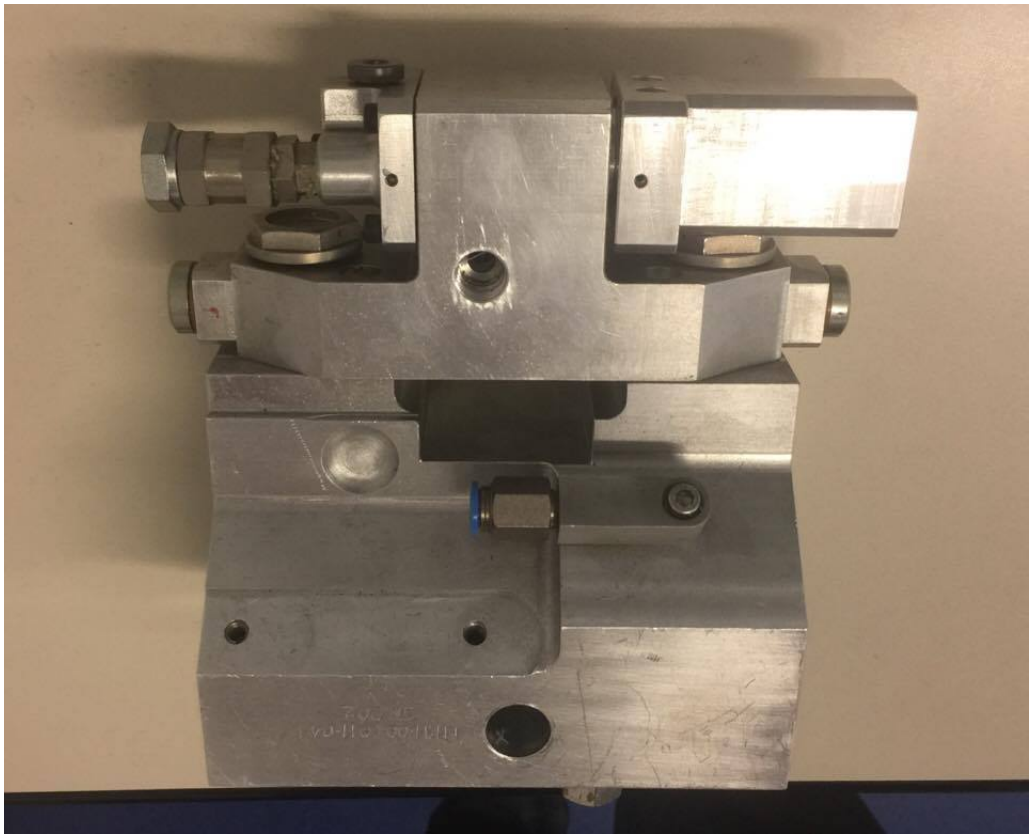

Figure 2.1: semi-active shock absorber built in Mechatronic Lab .

2.1 Model Description

Here we would describe the model that we have and present the each part of the prototype, (1) is the damper housing and it works like a passive damper,(2) is the manifold, this would link the damper from upper side and in that part we have the interesting component like the valve (2) and the inlet plugs as represented in (3) and other component we will represent them now, the spool (6) fit inside the sleeve (5) within these parts we can decide the state of the valve what ever it's close or open, the elastic joint (10) is linked to the electromagnetic actuator which is the (4) the brush less EC engine, (7) is the safety bar, the one return the valve into initial state, the spool is supported be bearing (11), (8)is the drain system when there is infiltration in the manifold and return them into chambers,(9) are the gefran pressure checked, all these components are represented in Figure2.2.

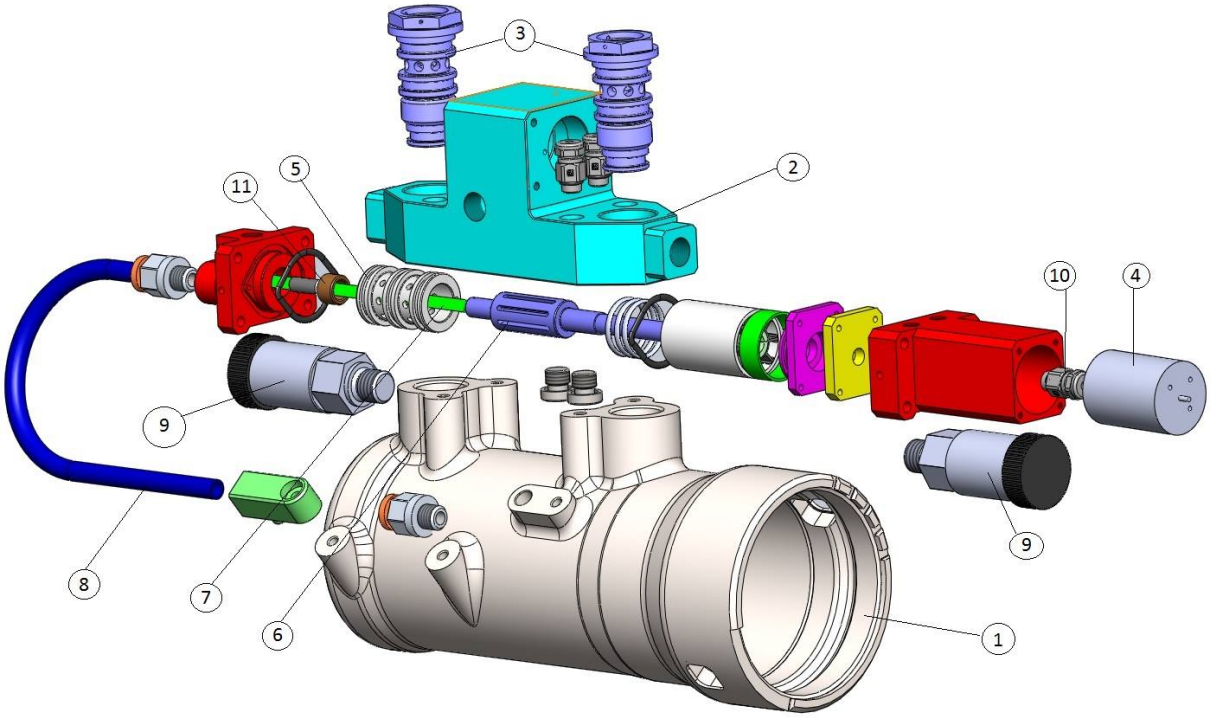

Figure 2.2: Exploded view of the active shock absorber .

In Figure 2.3 we can show the inward points of interest particularly with straightforwardness property so as to comprehend the model .we can control the gap of the valve by pivoting the spool inside the sleeve as should be obvious the Figure 2.4 ,the principle thought is that the valve goes into two states , open and close . when we open the valve we permit the fluid flow through the system in this action we reduce the damping characteristic, but if we close the valve we can the system would work like a passive damper and also we will have a high damping condition. we can control the damping force specially with this kind of valves, for example the partially open the high damping characteristic we get. in this model we can check the control range for damping characteristic and we can control the force that we need, all of these can be made by controlling the position of the spool by EC motor.

The benefit of using rotative valve rather than linear systems are presented in these points:

- the diverse sort of development the valve does not experience the inertia influence of the spool vibration.
- the range of control bandwidth is higher, and additionally its accuracy, since the spool situating can be accomplished through the established movement control of electric engines.

- the density power for the EC rotational motor is high.

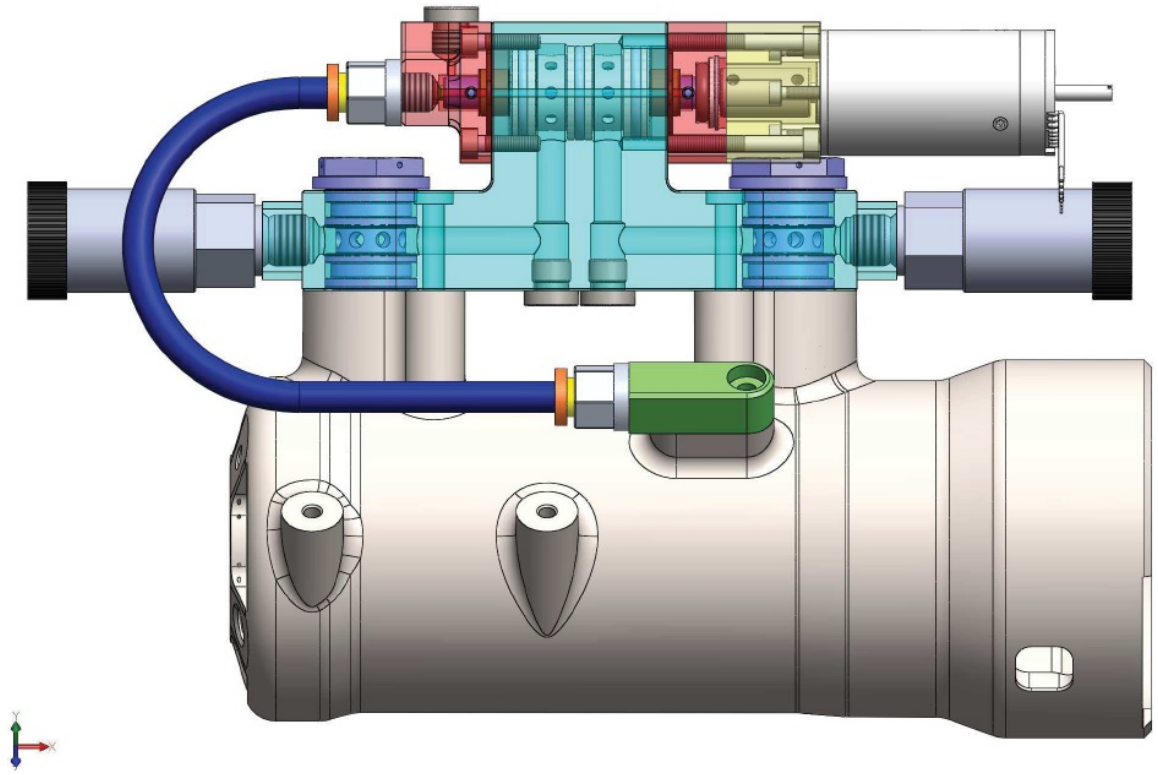

Figure 2.3: Overview of the assembled shock absorber.

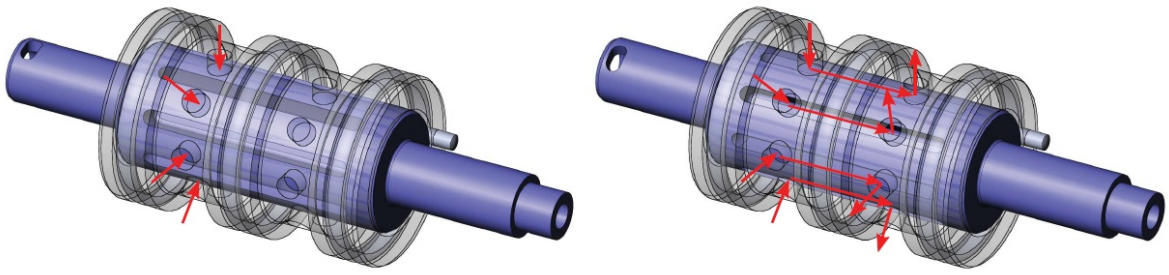

Figure 2.4: on the left full closed valve and on the right full open valve.

Chapter 3

Fluid Dynamics simulation and analysis

Initial studies were used COMSOL Multiphysics software platform for modelling and simulation the functioning of the valve. In this thesis we used PumpLinx®, it is a Computational Fluid Dynamics (CFD) tool, advance software which can provides accurate virtual testing for the analysis and performance prediction of fluid such as compressors, turbines, motors , pumps and valves. Where we will implement the prototype in the software and provide some simulation.

3.1 Import The Geometry

Firstly, to implement any geometry you need to import that form solidworks or any CAD programs, secondly , you need to split the parts from each other the specify the volumes of solid parts and the volume of fluid parts and the dynamic parts. Instead use these long methods, we try to do something smarter, moreover, we could skip the whole procedure, we could extract the fluid volume in the main part , where I mean in the spool and the sleeve in the manifold, this procedure can be done by solidworks, then we can implement this in PumpLinx software as shown in Figure 3.1

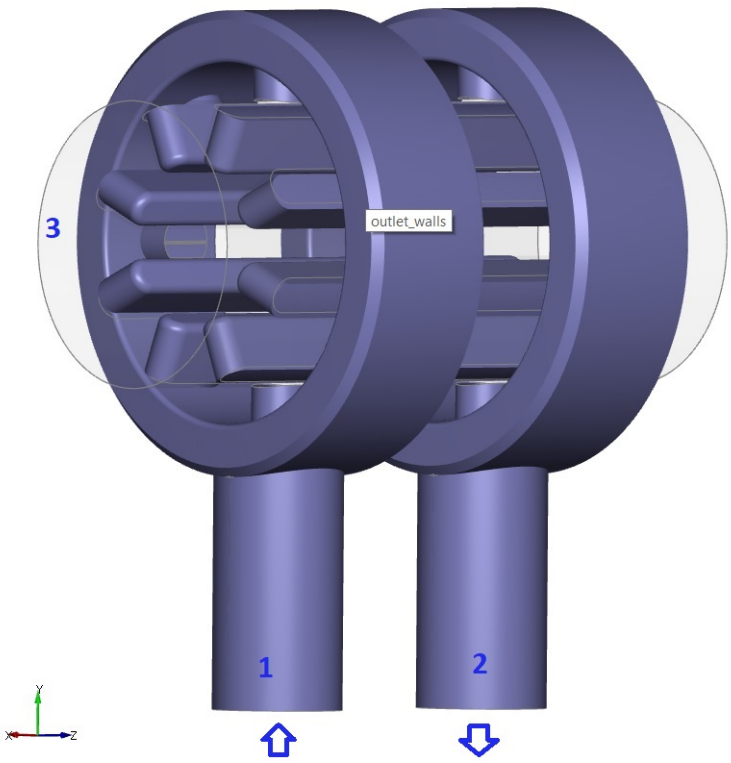

Figure 3.1: The simulation model that was inserted in PumpLinx software .

In this model describe the flow of fluid ,the entrance would be at number one , the fluid would be pass through the channels between spool and the sleeve as it shown in number 3 and the exit through number 2.

Assign to the state of the valve we can view whatever the valve is open or close or partially open as it shown in Figure 3.2

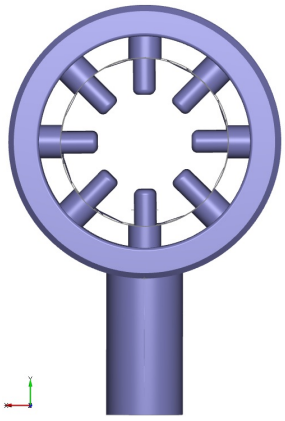

(a) fully open valve.

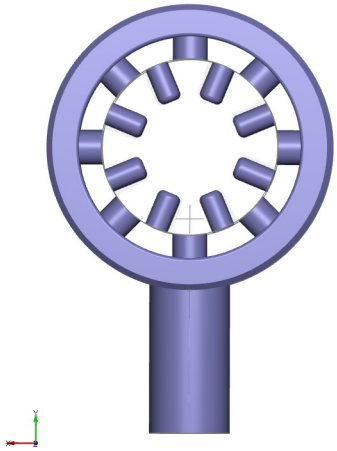

(b) fully close valve.

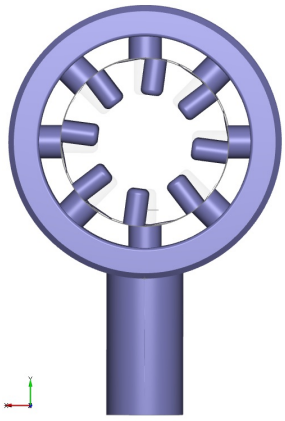

(c) partially open valve.

Figure 3.2: state of the valve

Lets start with the valve fully closed, in order to open the valve its enough to rotate the spool 22.5 degree, we will describe later in details the functioning of the model.

After implementing there are many things to prepare before we start simulation :

3.1.1 Prepare Surface

We apply some movement to define the surface of the geometry, The first step in creating these surfaces is typically to use a Boolean operation in the CAD software to extract fluid volumes , On the other hand , we start to split fluid volumes using projection of the sliding surfaces of the valve components as shown if Figure 3.3 and 3.4:

Figure 3.3: mgi of the channels

Figure 3.4: walls of the channel

in this Figure 3.3 represent the the boundaries of the channels or what they called mgi channels (Mis-matched Grid Interface) can be used to connect two Boundaries to create an Interface between the cells on either side. Any Boundary cell faces that do not match within a specified tolerance retain the properties of the original Boundary. In Figure 3.4 represent the walls of the channels , and both mgi channels and the walls submit the close surface of the channels of the channels.

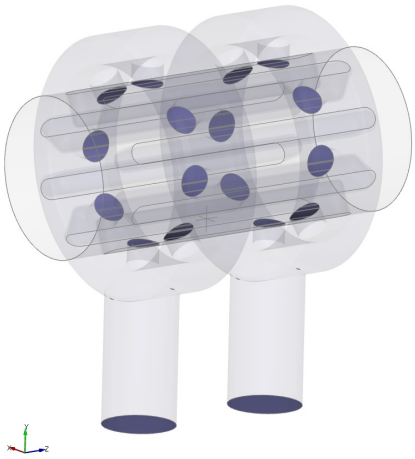

Figure 3.5: mgi of the channels

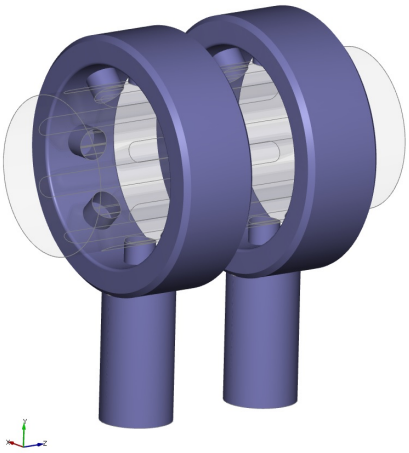

Figure 3.6: walls of the channel

As shown Figure 3.5 , the upper shaded surfaces represent the inlet mgi , the one could connect to the mgi channels , the lower shaded surfaces one of them represent the inlet of the fluid and the other is the outlet of the fluid. In Figure 3.6 shows the walls of the inlet and the outlet parts of the valve, merging together both figure6 and figure 7 submit the close surface of the Inlet and the Outlet.

3.1.2 Prepare Mesh

In this part we create mesh or grid, in Simerics/PumpLinx the mesh refers to a collection of points and lines that define the Volumes (2D or 3D) and Boundaries used by the numerical solver. The mesh in Simerics/PumpLinx is unstructured and supports arbitrary polyhedral mesh cells. In other words it transform the closed surface that win mentioned it into volumes that allows the program to identify them as shown in Figure 3.7 and 3.8.

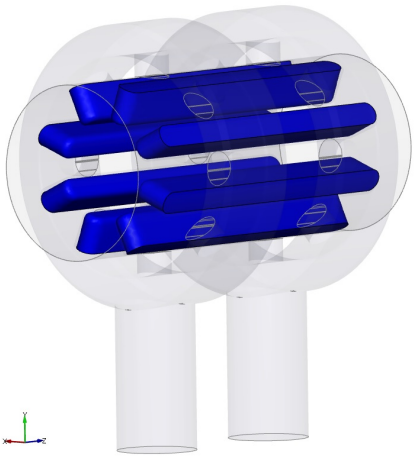

Figure 3.7: volumes of the channels

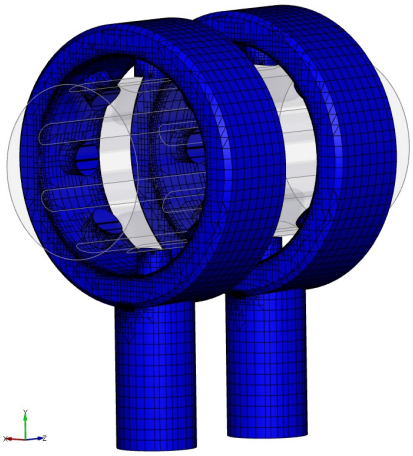

Figure 3.8: volumes of the inlet and the outley

While we create the volumes we could specify the geometric properties for each mesh, for example In Figure 3.7 we chose 30 degree as critical edge angle, 35 degree as curvature resolution , 0.05 asthe minimum cell size and 0.001 as the maximum cell size.

In Figure 3.8, we use general mesher to create the volumes of the inlet and the outlet parts, the geometric properties are the same that we used in channels volumes as well .

In Figure 3.9 represent the clearance surface , the one which connect the inlet and outlet from one side into channels the other side, this mesh has been built using template mesh , in the geometric properties we chose Annulus as a shape for the clearance, 360 degree as a pie angle, 0.0077m and 0.007715m for inner and outer radius , at the end we put 60, 3 and 100 as number of grid in 1st and second and third direction.

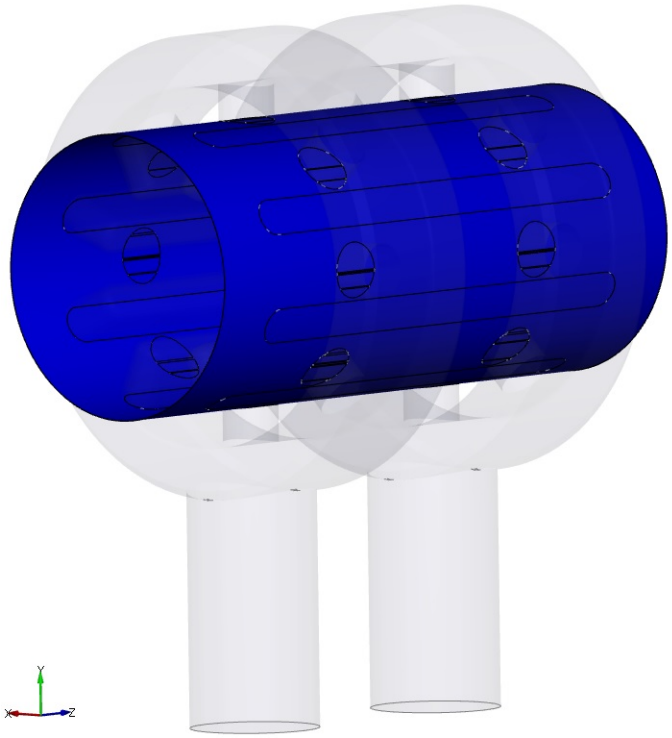

Figure 3.9: The clearance layer .

3.1.3 Prepare Model

In this part we are interesting to connect mgi parts with each other, furthermore in this part we are able to control the state of the valve , in other words in this part where we can open or close the valve ,regulate the fluid properties such as density and viscosity and prepare to start simulation as shown in Figure 3.10.

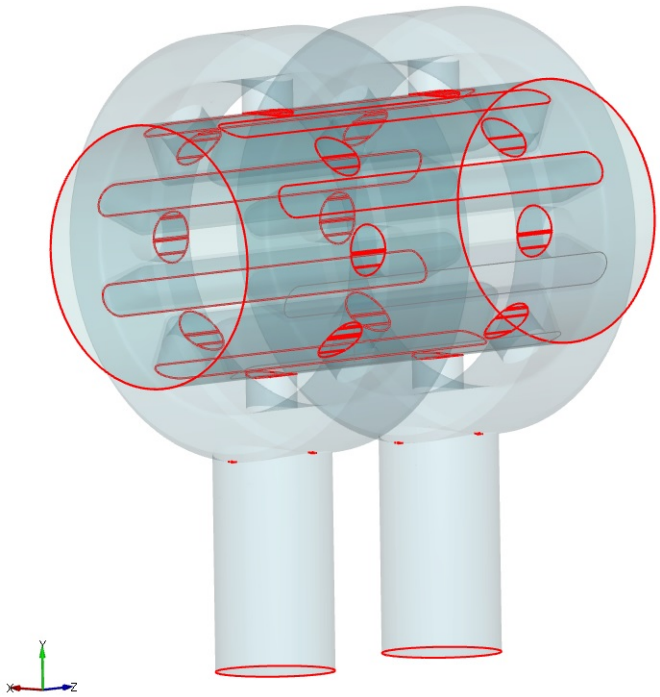

Figure 3.10: the interested mgi's.

3.2 Apply The Simulation

The simulation was applied by measuring the volumetric flow rate at the outlet port in different stages. That is to say, the volumetric flow rate was measured with different values of delta pressures at the ports and different aperture angle. We will describe later in details the input values. As you can see in this Figure 3.11 , the volumetric flow rate was calculated at outlet (that shaded area).

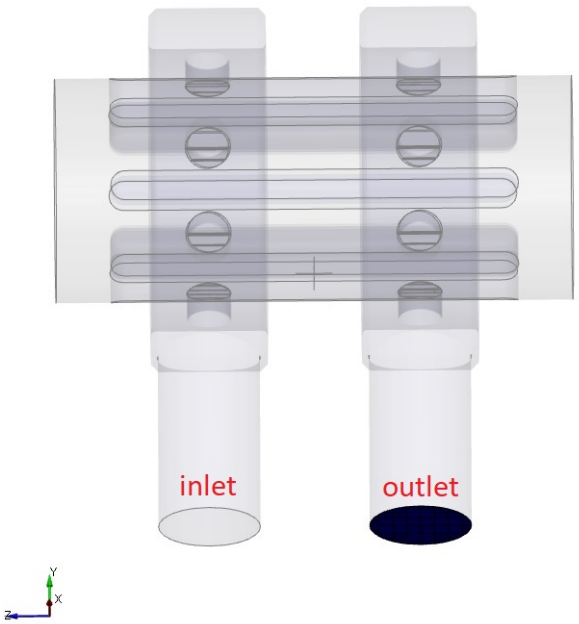

Figure 3.11: the interested mgi's.

3.2.1 Simulation Inputs

Before start we need first assign the input values, from the geometry description the diameter of the inlet and the out ports its d=7 mm, the area of cross section $A_p = 0.0004mm^2$, the maximum fluid velocity $V_{max} = 2m/s$, the maximum mass flow rate $Q_{max} = V_{max} * A_p = 8e-4m^3/s$.

Another key thing to remember , the maximum drop pressure $\Delta P_{max} = 40bar$, the force $F = \Delta P_{max} * A_p = 1.6kN$, the pressure outlet must be always fixed $P_{outlet} = 2bar$. we should regulate the inlet pressure accord this formula $P_{inlet} = P_{outlet} + \Delta P$, the ΔP will take these values (4 8 12 16 20 24 28 32 36 40)bar, last and not least the aperture angle would start from 0 (where the valve fully open) to 22.5 (where the valve fully close) , increasing the aperture angle 2 degree for each simulation , in other words we would calculate the volumetric flow rate at the outlet port for each aperture angle θ= (0 2 4 6 8 10 12 14 16 18 20 22.5)° and for each ΔP.

3.2.2 Simulation Results

After having characterized the material, the next step is to start simulation and analyse the results, in the next Table 3.1 you can find the measuring that we applied .

θ/ Δ p	4	8	12	16	20	24	28	32	36	40	bar
0	0.000432	0.000621	0.000766	0.000888	0.000995	0.001094	0.001185	0.001269	0.001348	0.001422	
2	0.000426	0.000612	0.000754	0.000875	0.000981	0.001077	0.001166	0.00125	0.001328	0.001401	
4	0.000408	0.000586	0.000723	0.000837	0.000939	0.001031	0.001116	0.001195	0.001271	0.001342	
6	0.000384	0.000551	0.000679	0.000787	0.000882	0.000969	0.001048	0.001122	0.001192	0.001259	
8	0.000343	0.000493	0.000607	0.000703	0.000787	0.000865	0.000935	0.001002	0.001065	0.001124	
10	0.000288	0.000415	0.000512	0.000596	0.000669	0.000735	0.000795	0.000852	0.000905	0.000956	
12	0.000214	0.00031	0.000384	0.000446	0.000499	0.000549	0.000595	0.000638	0.000678	0.000716	
14	0.000135	0.000194	0.000243	0.000283	0.000316	0.000351	0.000378	0.000405	0.000431	0.000457	
16	6.17E-05	9.09E-05	0.000116	0.000135	0.000154	0.00017	0.000185	0.000197	0.000212	0.000223	
18	1.97E-05	3.06E-05	3.97E-05	4.87E-05	5.78E-05	6.38E-05	6.85E-05	7.29E-05	7.89E-05	8.39E-05	
20	1.93E-06	2.31E-06	2.12E-06	2.65E-06	3.09E-06	4.25E-06	4.92E-06	6.81E-06	8.71E-06	1.05E-05	
22.5	5.38E-06	1.08E-05	4.92E-06	7.90E-06	1.23E+05	1.44E-05	1.75E-05	1.08E-05	1.68E-05	1.81E-05	m^3/s
degree(°)											

Table 3.1: volumetric flow rate at the outlet

With these results we can analyze many things, firstly , the volumetric flow goes spontaneously every time we change the any parameter, for example at a fix aperture angle , every time we increase the delta P the volumetric tense to increase as shown in depicted Figure 3.12.

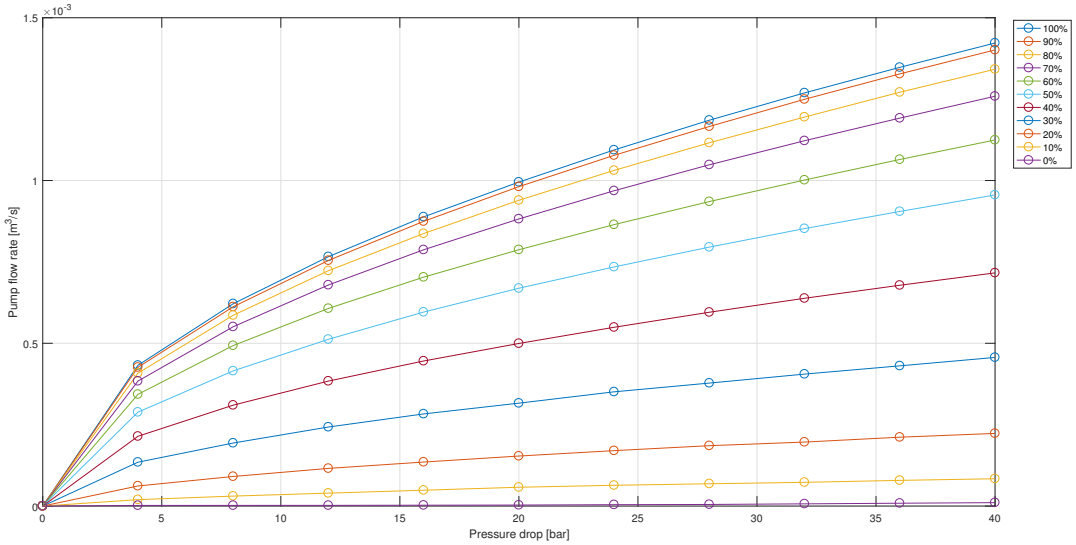

Figure 3.12: volumetric flow rate as function of ΔP [bar].

on second hand, Every time we increase the aperture angle (turn to close the valve) the volumetric turn to decrease as shown in depicted Figure 3.13.

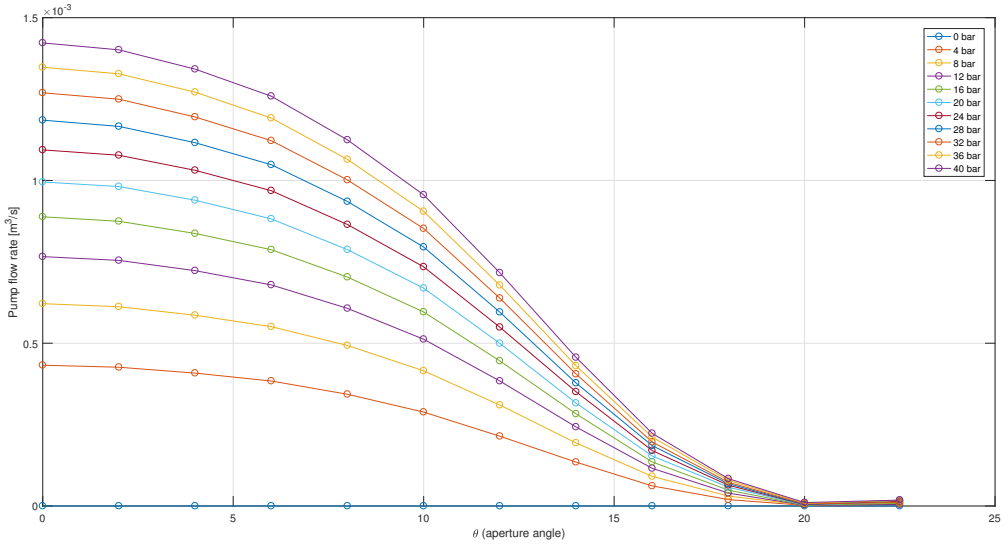

Figure 3.13: volumetric flow rate as function of aperture angle θ [degree].

However, these studies can provide us the measurement of the simulation, which can tell us that the fluid goes spontaneously and we get reasonable results, here we can see the overall view the 3d graph of the simulation (shown in Figure 3.14.)

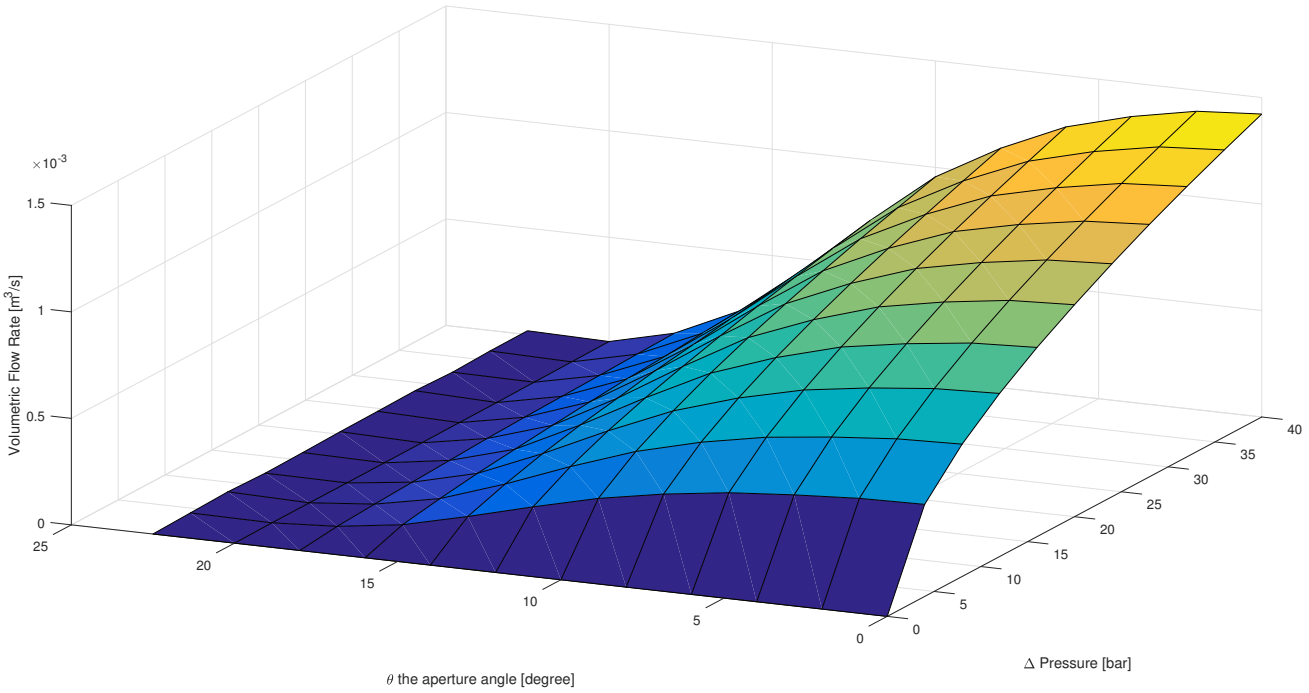

Figure 3.14: three dimension graph of simulation .

3.2.3 Drawback and Limitation

During the simulation there are some critical point where were the volumetric flow rate has been unreasonable , specially , at these points where the aperture angle 20 and 22.5 as you can see the Table 3.1, we can check that the aperture angle from 0 degree to 18 degree the flow rate increase monotonically unlike at these two aperture angle , maybe this behaviour because the flow in turbulence state, we will check later check Equation 3.1 page 30,or miss estimate the number of grid in 1st or 2nd direction in clearance layer (was explained in chapter prepare mesh), the second method wasn't useful no manner how many time we change the number of greed ,to that end, it lead us to the only cause the turbulence (shown in Figure 3.15).

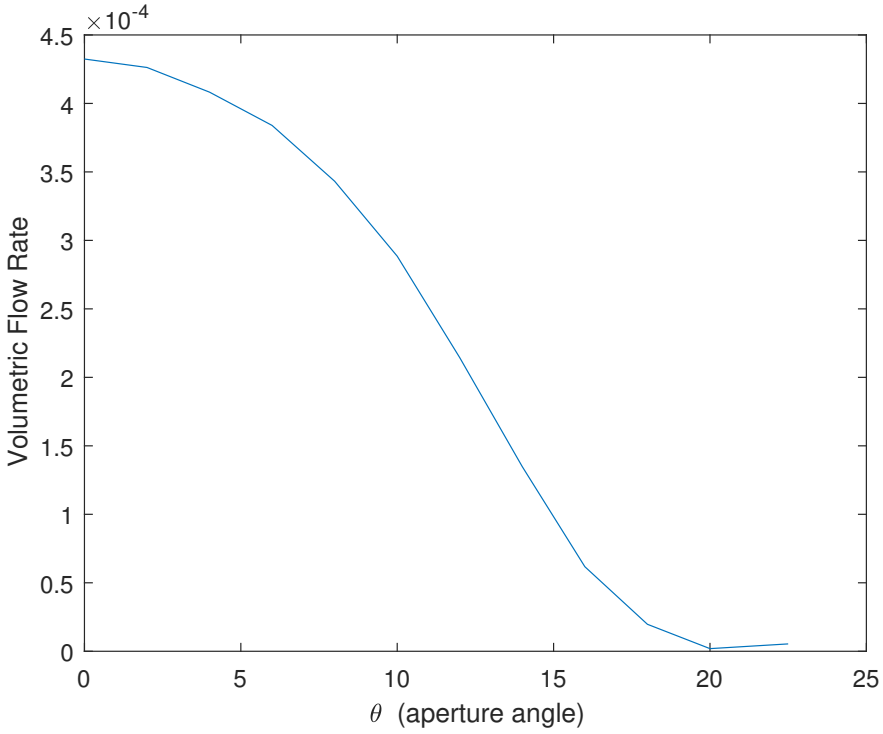

Figure 3.15: volumetric flow rate at different aperture angle at fixed ΔP.

In the graph we can observe the values of flow rate through all aperture angle at fixed ΔP, repeat the procedure with all ΔP and we would face the result the miss-order of flow rate at angle 20 and 22.5, where it suppose to be monotonically decreasing. In order to display the depicted up there , I have approximated some values in a way doesn't affect the overall results .

Reynolds number: regards to sleeve and spool graphs, the daiameter of the sleeve 15.4(+0.02 +0.03)mm and for the spool 15.4(0 -0.01)mm so:
$D_{out} = 15.4 + 0.015 = 15.4150mm = 0.015415m$
$D_{in} = 15.4 - 0.005 = 15.395mm = 0.015395m$

From the simulation$Q = 2.31e - 6$, where we can see irregular flow rate.
$Q = \frac{v*\pi*D^2}{4} \Rightarrow v = \frac{Q*4}{\pi*(D_{out}^2 - D_{in}^2)}$ $v = 4.7731m/s$

$$\mathbf{Re} = \frac{\rho * v * l}{\mu} = \frac{836 * 4.7731 * 0.0345}{0.01} = 13766.575 \tag{3.1}$$

ρ=fluid density v=fluid velocity l=spool length μ=dynamic viscosity .
Its much bigger than 2300 so its for sure in turbulent state.

Chapter 4

Experimental And Simulation Results

In this chapter we will present and discuss experimental and simulation results, comparing the results in order to calculate the error that match the specific description, the experimental results were took from previous studies done by Ing. Andrea Vellante [5] , and the simulation part done by us using PumpLinx.

4.1 Equipment Definition

In Figure4.1 show the tools that have been utilised in this experiment, also in this Figure it demonstrates the gadgets in which we used to derive and control the pump of the hydraulic circuit and the EC engine as well. As you can see the inverter (1) that supply the electric energy and also to the computer portal (2) where in this device we are able to angular velocity of the electric motor. Through The GUI program installed on the second computer as it shown in (3), and that is Linked to MPPM in (5) through a CAN network (4), the (5) was powered by a power supply unit (6). (7) is the USB device that power the digital oscilloscope in that the the delta pressure has been manged in the valve. The pump that we used (8) , and the reservoir of the fluid (9) has been presented in Figure 4.2, also we can see our prototype (10). In Figure 4.3 we can check the sensor assembled in the prototype by the mainfold. The hole procedure has been done in the laboratory of Mechatronics at the Varese where there is another department of the Politecnico di torino.

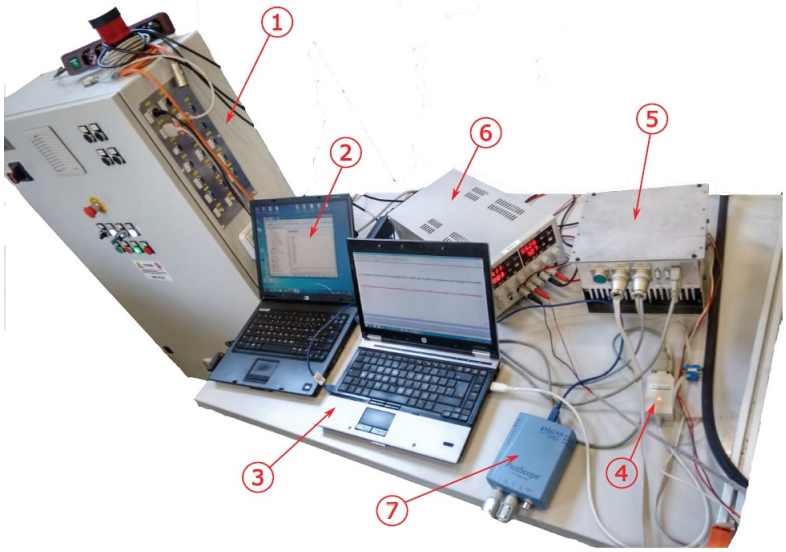

Figure 4.1: Electronic equipment of the test rig [5].

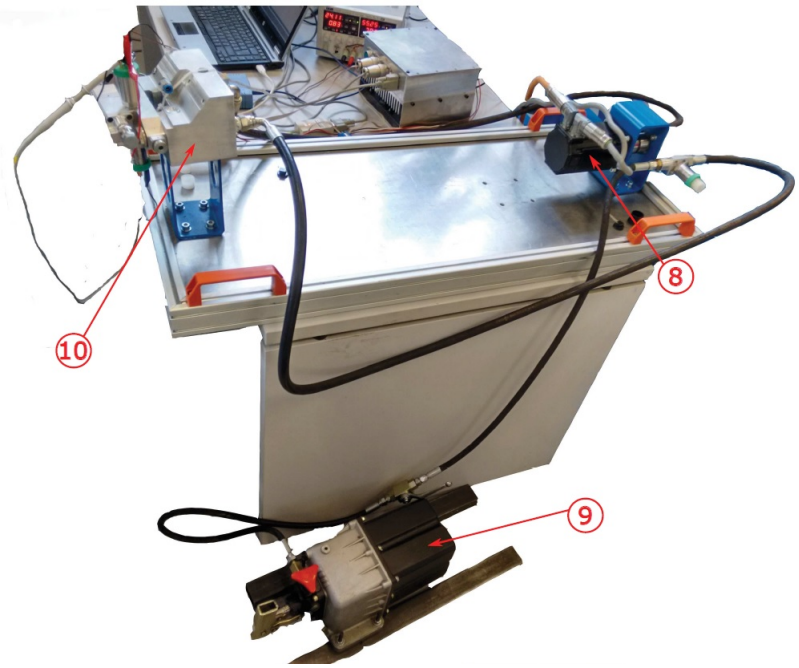

Figure 4.2: Hydraulic equipment of the test rig [5].

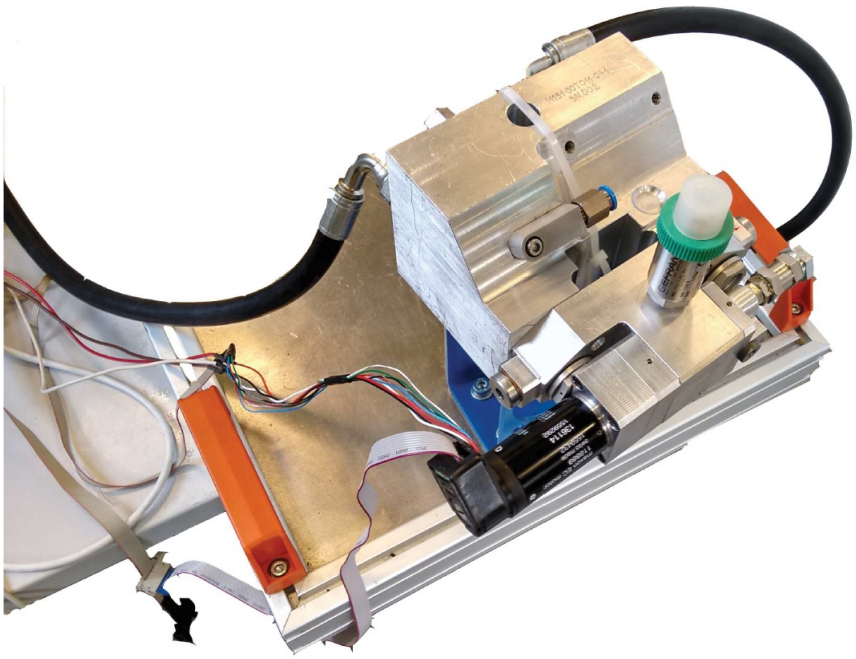

Figure 4.3: Close-up on the valve prototype [5].

4.2 Preliminary operations

This part of Preliminary operation and the next part the Experimental results has been observed and monitored by ing. Vellante and the assistant of this thesis, my work is to contribute and compare the simulation result with the experimental one, so I thought it's necessary to present these parts from previous Thesis. "Before taking any measurement, possible mechanical and electrical working issues have been investigated. For this purpose, the valve assembly has been subjected to short running-in phases at different angular speeds. Despite the fact that the spool seemed to follow quite accurately the reference speed in a short time, some problems in the start-up phase have arisen: in particular some stick-slip phenomena have occurred at low speeds, which are symptomatic of an excessive static friction. This may be due to the gasket seals that, because of their elastic nature, are deformed by the pressure of the preloaded fluid and therefore they are pressed against the spool shaft. Additionally, in some angular sectors the spool got stuck and the rotation started only with high peaks of current, condition that should be avoided to preserve the integrity of the motor windings. Due to the numerous variables that influence the static friction (such as the preload pressure, the manufacturing tolerances, the temperature, and so further), it is very difficult to quantify the related coefficient. A different matter is the evaluation of the viscous friction coefficient: once the motor is

actuated and the angular speed is imposed, the related motor current can be measured. Knowing that $Te = K_m * i = c_s * \omega$, the torque generated by the motor can be easily computed and plotted with respect to the angular speed, such as depicted in Figure 4.4. The operation is then repeated with different fluid preload pressures, to have a more precise characterization of the coefficient, which is the slope of the linearized curves. The resulting mean value of the coefficient is $8.166 * 10^{-4} Nmsrad^{-1}$ which can be considered acceptable since it sums up several friction phenomena, such as the fluid film between the spool and the sleeve or the contribution of the bushes. The position and speed controller gains have been consequently updated and adapted to the actual electrohydraulic system configuration."[5]

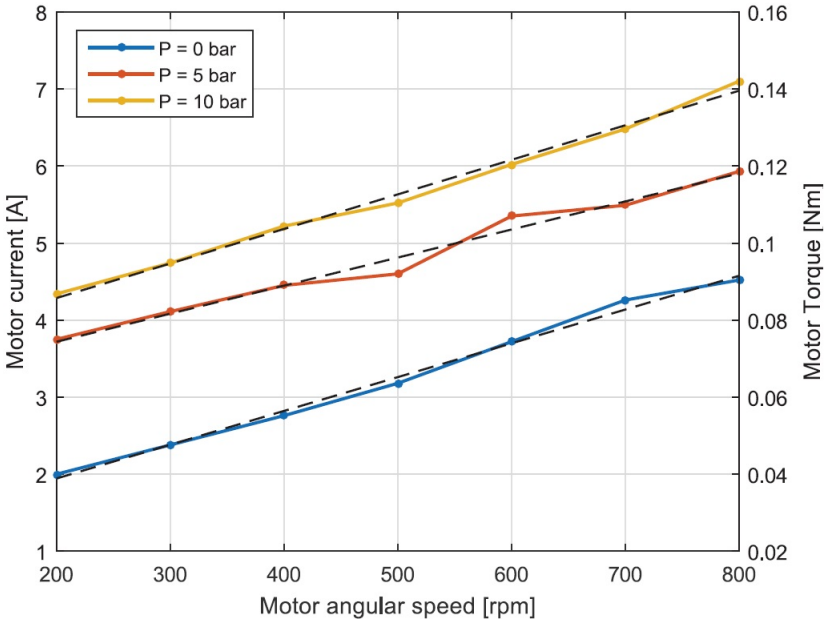

Figure 4.4: Viscous friction characterization [5].

4.3 Experimental results

Vellante observation "With the test rig correctly configured and tested, it has been possible to proceed in the characterization of the valve, with the main focus to evaluate the pressure drop corresponding to different opening percentages. The experimental curves are taken according to the following process:

- 1. The fluid circuit is preloaded with a pressure of 10 bar and the spool is rotated to a precise angle defined through the notebook (3).
- 2. The pressure differential is firstly measured with the pump in idle condition by means of the pressure sensors connected to the oscilloscope. The

voltage read on the software interface of the latter is indeed proportional (e.g. $50Vbar^{-1}$) to the pressure on the ducts of the manifold1.

- 3. The pump is actuated and its speed regulated by means of the notebook (2): knowing the displacement of the pump $D_p = 3.39 * 10^{-7}m^3$, the angular speed n (in rpm) is proportional to the volumetric flow rate Q according to the formula 4.1

$$Q = \frac{\pi * 2}{60} * n * D_p \quad \left[\frac{m^3}{s}\right] \tag{4.1}$$

- 4. The measurements are repeated for increasing speeds, until the pump limit is reached.

For what concerns the last point, the maximum speed reached by the pump before entering the protection mode was 5000 rpm, corresponding to a flow of $1.78{*}10^{-4}m^3s^{-1}$ that is quite limited compared to the rates investigated through software simulation. The process described above is repeated for different spool angles so that the various curves can be reproduced as it is depicted in Figure 4.5 Being known the piston area A_p, it is possible to plot the damping characteristic for several stroke velocities, whose value is defined as $v_p = Q/A_p$. The resulting plot is shown in Figure 4.6.

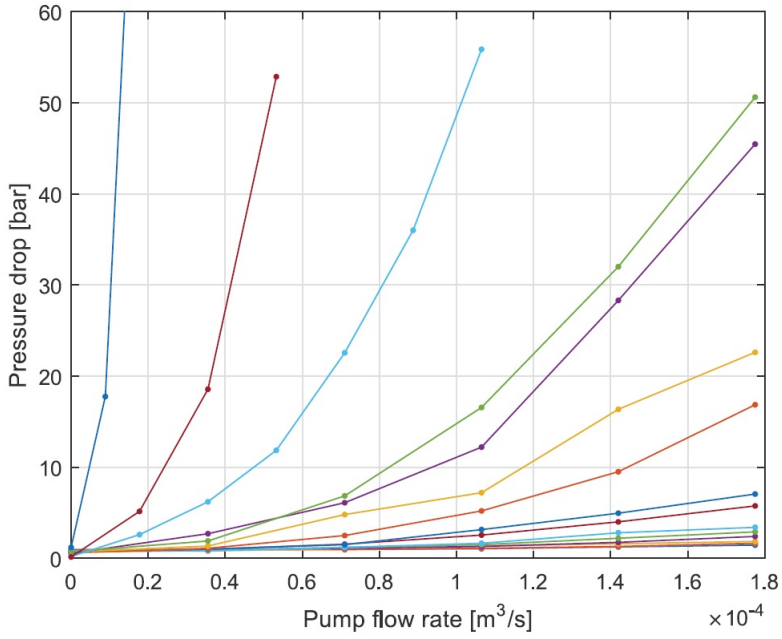

Figure 4.5: The dots that match the lines represent the experimental flow rate as a function aperture angle and pressure drop, these measurement from the dots were took form a sensor placed in the model [5].

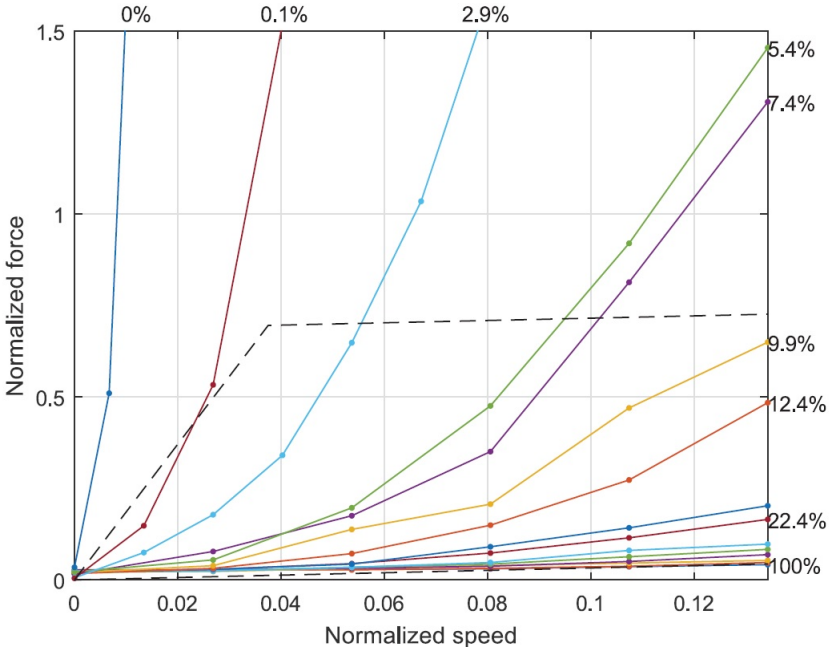

Figure 4.6: Experimental damping characteristic developed by the valve assembly for different opening percentages [5].

In Table 4.1 the simulation runs performed are resumed along with the spool rotation angle and the opening percentage of the valve. It can be noticed that the relationship between the two differs from what was described in figure 2.16. This may be due to spool misalignments and/or to manufacturing tolerances. In the last column of the same table it is reported the maximum force over maximum speed for the characteristic analyzed: it would be the slope of the line between the zero and the highest point of the characteristic, that is a sort of equivalent damping coefficient.

Table 4.1: Summary table of the test runs, the related opening percentage and the maximum force over velocity ratio.

Run	Angle	Opening %	F/V ratio $[\mathrm{kN}sm^{-1}]$
1	1°	94.99	8.9
2	5°	74.97	10.2
3	10°	49.95	11.4
4	12°	39.94	14.8
5	13.5°	32.43	17.9
6	14.4°	27.93	20.9
7	15.5°	22.42	35.4
8	16.3°	18.42	43.4
9	17.5°	12.41	103.8
10	18°	9.91	139.2
11	18.5°	7.41	279.9
12	18.9°	5.41	311.6
13	19.4°	2.9	573.2
14	20°	0.1	1084.8
15	20.5°	0	5726.5

It can be immediately noticed that closing the valve, the F/V ratio increases exponentially, and tends to infinite for the full closed condition. This reflects the valve behavior when it is assembled to the damper cylinder, since the pressure on a side of the spool would be very high, and vice versa on the opposite inlet. The overall behavior is represented in Figure 4.7, where the F/V ratio is plotted according to the opening percentage."[5]

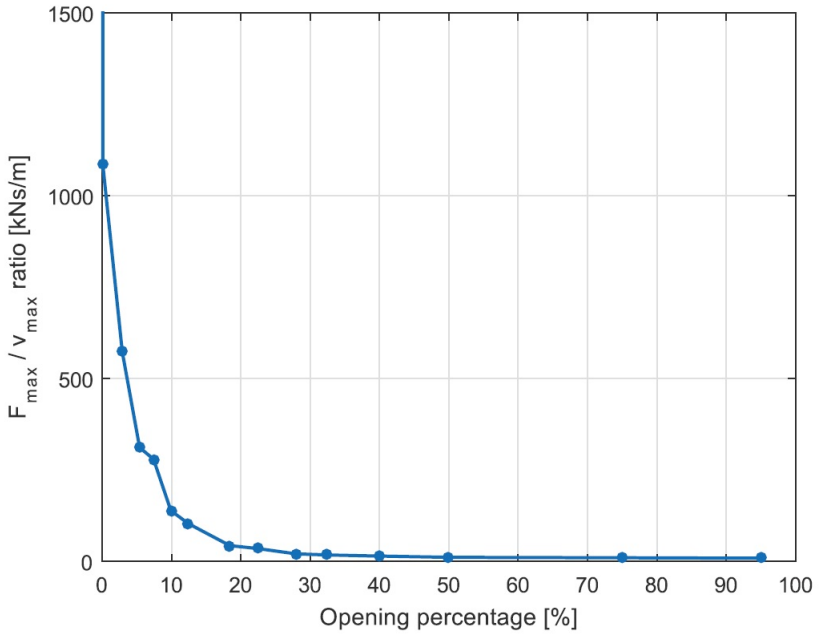

Figure 4.7: F_{max}/v_{max} ratio trend according to the valve opening percentage [5].

4.4 Results comparison (experimental - simulation)

The aim of this comparison is to calculate the difference (error) between experimental and simulation results by obtaining the experimental flow rate (Q_{exp}) from the exponential curves in the measured points (as shown in Figure 4.5), and interpolate the results from the simulation that matches both aperture angle and $\Delta pressure$, we will check that in details.

In Figure 4.8 it has been presented the measurement of experimental and the simulation, the straight lines show the experimental measurement and the red circles show the simulation ones.

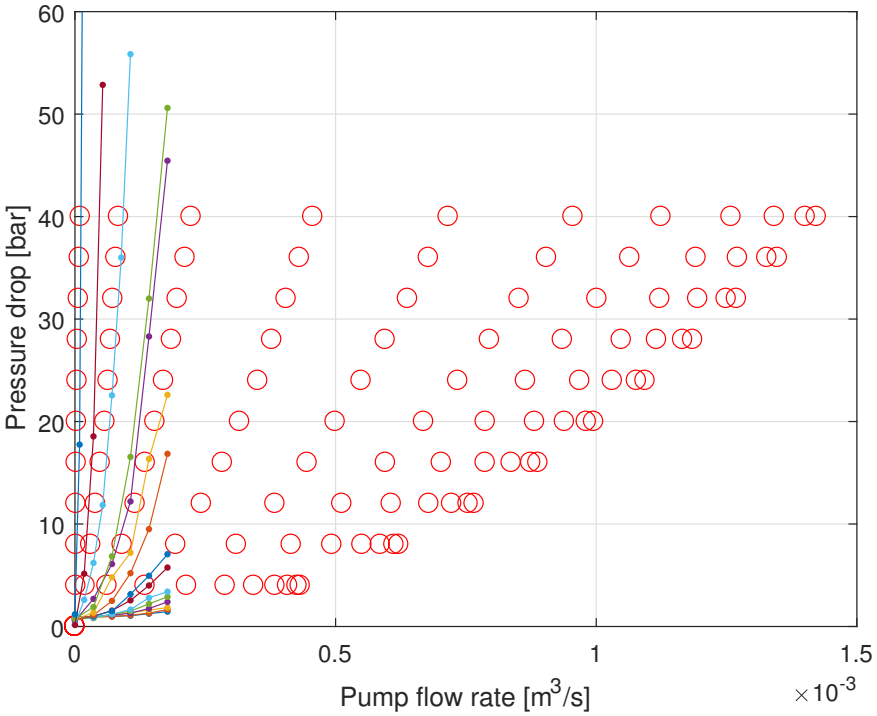

Figure 4.8: experimental and simulation flow rate measurements.

In order to compare each sequence of the measurements, griddedinter- polant was applied to the Matlab code ,so it is easy to check the similarity, each exponential line has its own aperture angle as you can see at the labels,check the Figure 1.10. As you can see this figure the error is high at some cases, our goal after doing the comparison is to reduce the error as much as we can. So applied three different methods comparing the experimental and the simulation result, first method is to compare the matched aperture angle and we found the amount of error high, second method is to eliminate the offset error form the ex-experimental result then we compare the graphs that matched the same aperture angle and we found the error still high,third method aim first to eliminate the offset error , second to compare each experimental with nearest simulation one, with the last method we are able to reduce the error in the most cases ,so the comparison would follow the last method, Figure 4.9 will explain how the third method has been done.

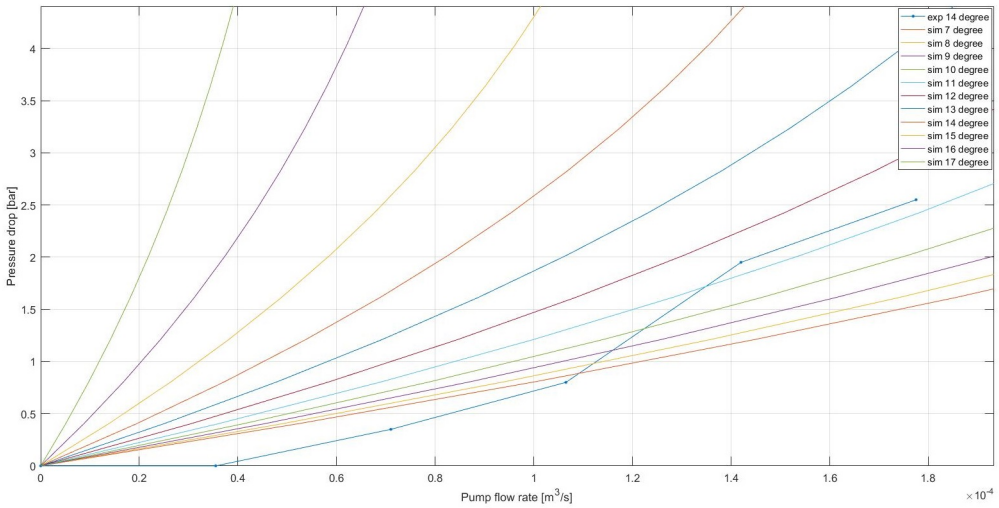

(a) compare experimental 14 degree and all curves

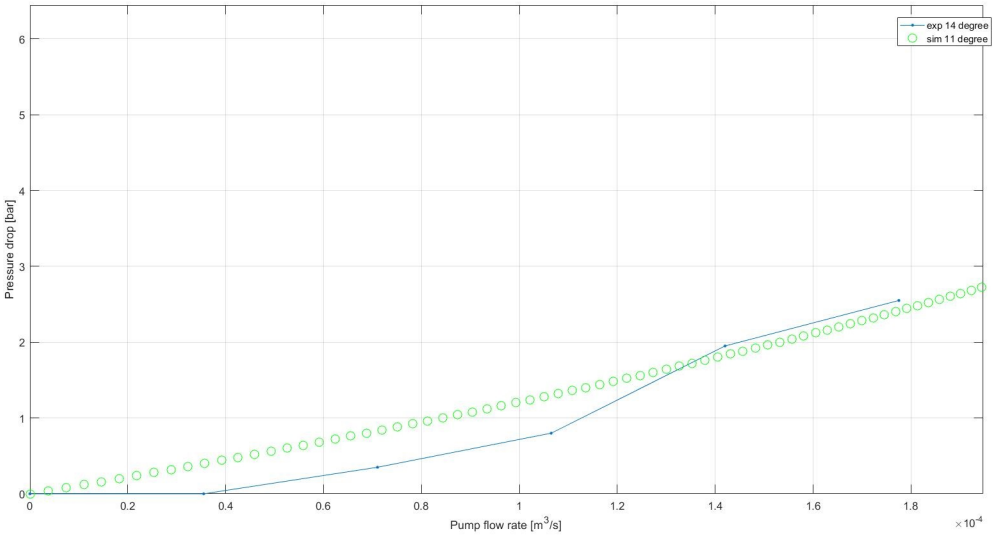

(b) compare experimental 14 degree and simulation 11 degree

Figure 4.9: An example of using the Third method, for instance we took the state where the (experimental curve at 14 degree) then we compare it with all the simulation one, then we picked up the nearest one which its (simulation 11 degree) in our state, then we calculated the error

In Figure 4.10 we illustrated the comparison for the most of our cases, showing the nearest curve in order to reduce the error.

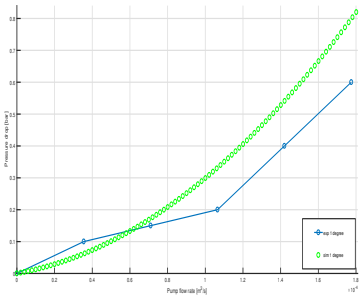

(a) exp 1° and sim 1°

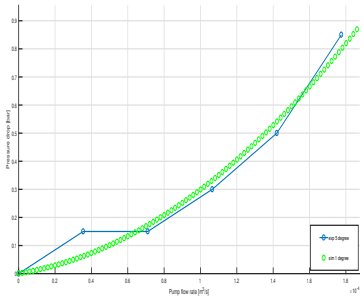

(b) exp 5° and sim 2°

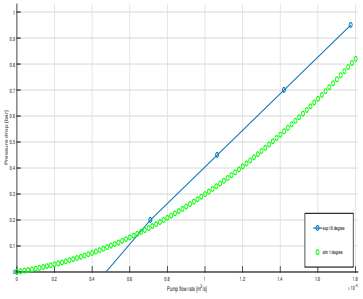

(c) exp 10° and sim 2°

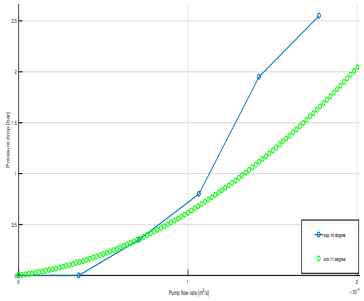

(d) exp 14° and sim 11°

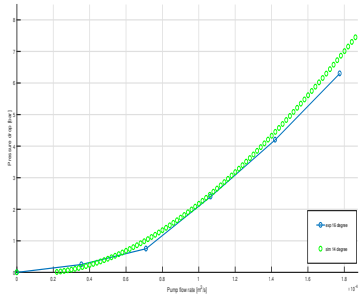

(e) exp 16° and sim 14°

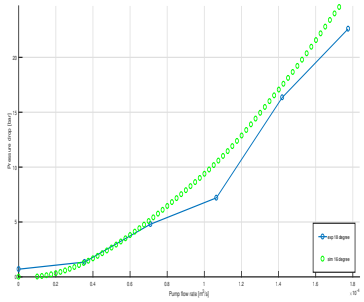

(f) exp 18° and sim 16°

Figure 4.10: The result of the comparison using the Third methode

Before we move to the final results, we need to mention the procedure that we followed to get the results, To give an illustration of what I mean, let's look at the case where the aperture angle it is 18° (20% open) as shown in Figure 4.11.

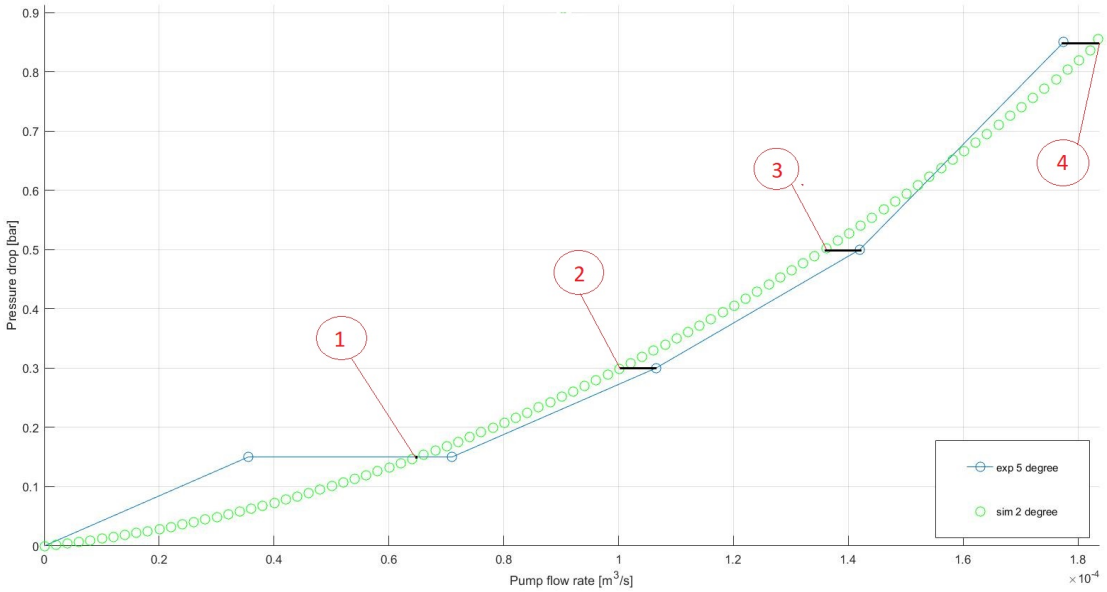

Figure 4.11: The flow rate at following marked number are: ①0.000038, ②0.000038,③ 0.0000511, ④0.0001086, ⑤0.0001836

In the Figure 4.10,firstly, each of the experimental and the simulation have different aperture angle ,secondly, we put a horizontal line connect the experimental line with the simulation one, to that end, both connected points have the same pressure drop. with this procedure we are able to extract the flow rate,by applying this concept to all cases of the model, then we are able to calculate the error between experimental and simulation results as shown in Table 4.2 and 4.3. This approach were done to the closest behavior between the experimental and the simulation results. Refer to the result that we have from the Tables we can realize the error is a little bit height at the small aperture angle, the cause of these height error refer to inaccurate observation during the experimental tests, but at the same time we can see at the high aperture we have almost matched results as we can see from Table 4.2 and 4.3 and the Figure 4.10.

Table 4.2: Error measurement.

Experimental		
apreture angle(Θ)	Delta pressure(ΔP)	volumetric flow rate (Q_{exp})
[degree°]	[bar]	[$\frac{m^3}{s}$]
1	0.95	3.55E-05
1	1	7.10E-05
1	1.05	0.0001065
1	1.25	0.000142
1	1.45	0.0001775
5	0.95	3.55E-05
5	0.95	7.10E-05
5	1.1	0.0001065
5	1.3	0.000142
5	1.65	0.0001775
10	0.8	3.55E-05
10	1.1	7.10E-05
10	1.35	0.0001065
10	1.6	0.000142
10	1.85	0.0001775
12	0.95	3.55E-05
12	1.1	7.10E-05
12	1.3	0.0001065
12	1.75	0.000142
12	2.4	0.0001775
14	0.85	3.55E-05
14	1.2	7.10E-05
14	1.65	0.0001065
14	2.8	0.000142
14	3.4	0.0001775
16	1	3.55E-05
16	1.5	7.10E-05
16	3.15	0.0001065
16	4.95	0.000142
16	7.05	0.0001775
18	1.35	3.55E-05
18	4.8	7.10E-05
18	7.2	0.0001065
18	16.35	0.000142
18	22.6	0.0001775
20	5.15	1.78E-05
20	18.55	3.55E-05
20	52.85	5.33E-05

Table 4.3: Error measurement.

Simulation			
nearest (Θ)	nearest (ΔP)	match (Q_{sim})	Error
[degree°]	[bar]	$[\frac{m^3}{s}]$	$[1 - \frac{Q_{sim}}{Q_{exp}}]$
1	0.9498	0.00001884	4.69E-01
1	1	0.00002503	6.47E-01
1	1.05	0.000036115	6.61E-01
1	1.25	0.00006113	5.70E-01
1	1.449	0.00008994	4.93E-01
2	0.9503	0.00002503	2.95E-01
2	0.9503	0.00002503	6.47E-01
2	1.1	0.0000492	5.38E-01
2	1.3	0.00007855	4.47E-01
2	1.65	0.000124	3.01E-01
2	0.8004	0.0001171	-2.298591549
2	1.1	0.00003115	5.61E-01
2	1.35	0.000064	3.99E-01
2	1.6	0.0001067	2.49E-01
2	1.85	0.000139	2.17E-01
5	0.9504	0.000038	-7.04E-02
5	1.1	0.00002311	6.75E-01
5	1.3	0.0000511	5.20E-01
5	1.75	0.0001086	2.35E-01
5	2.4	0.0001836	-3.44E-02
11	0.8496	0.000036	-1.41E-02
11	1.2	0.00003227	5.45E-01
11	1.65	0.00006875	3.54E-01
11	2.801	0.0001507	-6.13E-02
11	3.4	0.0001858	-4.68E-0
14	1	0.00001176	6.69E-01
14	1.5	0.00003534	5.02E-01
14	3.15	0.0000947	1.11E-01
14	4.949	0.0001389	2.18E-02
14	7.051	0.0001724	2.87E-02
16	1.351	0.0000364	-2.54E-02
16	4.801	0.00006801	4.21E-02
16	7.201	0.00008451	2.06E-01
16	16.35	0.00013685	3.66E-02
16	22.6	0.0001644	7.38E-02
19	5.154	0.0000232	-3.07E-01
19	18.53	0.00005481	-5.44E-01
19	52.85	0.00009141	-7.17E-01

Chapter 5

Motor Control

There is no suspicion that if we want to control the entire system we need focus on the angular rotation of the spool valve. since we are working in the system at different pressure drop for specific angle, so these variables should be accurately manged, for the required damping characteristic. The modification of the angular position should be quick as conceivable to have a speedy reaction across the system in time limit around 10 milliseconds. So we have to be more accurate while we design a control and the response should be fast enough. In this part we will simulate the system through Simulink and Matlab.

5.1 Dynamic model

The electromechanical system consist of four sections: the electrical motor, spool, the flexible joint that connections them and safety bar. The first one is brushless DC motor produced by Maxon (swiss company), the electric circuit that show the inside function as it shown in this depicted 5.1. as we can see we insert the amount of voltage that we need to winding terminals then permanent magnet (rotor) start to rotate, this will generate a Torque T_e and a EMF which is relative to a constant like it shown in the next equation:

$$E = K_v \omega_m \qquad T_e = K_m I$$

The two constants introduced above have a similar weight cleared in unlike units of estimation, they are connecting the component between the mechanical and electrical feature of the actuator. The previous can be checked by placing Kirchoff's voltage law in the circuit as shown:

$$V = RI + L\dot{I} + K_v \omega_m \tag{5.1}$$

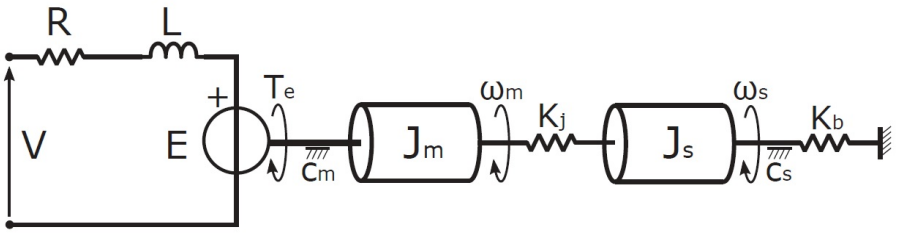

Figure 5.1: Equivalent model of the electromechanical system consisting in the motor, the elastic joint, the spool and the torsion bar [5].

The description and the explanation of the circuit and the following equations made by ing. Vellante in previous studies: "Being the motor a three-phase system, R and L are respectively the resistance and the inductance between two of the three phases, since for each instant two of them are on while the remaining is off; for this reason they are also known as "phase to phase" quantities. From the mechanical point of view, the motor torque must win at first the inertia J_m of its own rotating parts, the viscous friction c_m in the shaft bearings and then the generic resisting torque T_r of the linked elements. Therefore, the force equilibrium can be described in this equation 5.2. Neglecting prima facie the effects of the torsion bar K_b, the components that the motor has to move are the joint, which contributes with its torsional stiffness K_j , and the spool, whose inertia J_s and viscous friction c_s torques are to be taken into account. As a consequence, the angular velocities of the spool and the motor ω are unlikely to be the same and, for a precise estimation of the resulting angular position of the spool θ_s, the overall electromechanical model must be studied."[5].

$$K_m I = J_m \dot{\omega}_m + c_m \omega_m + T_r \omega_m \tag{5.2}$$

Its expression will be:

$$\left\{ \begin{array}{c} V = RI + L\dot{I} + K_v \dot{\theta}_m \\ K_m I = J_m \ddot{\theta}_m + c_m \dot{\theta}_m + K_j(\theta_m - \theta_s) \\ J_s \ddot{\theta}_s + c_s \dot{\theta}_s + K_j(\theta_s - \theta_m) = 0 \end{array} \right\}$$

after we rewrite the equations in useful order:

$$\left\{ \begin{array}{c} \dot{I} = \frac{V - RT - K_v \dot{\theta}_m}{L} \\ \ddot{\theta}_m = \frac{K_m I + K_j \theta_s - c_m \dot{\theta}_m - Kj\theta_m}{J_m} \\ \ddot{\theta}_s = \frac{-c_s \dot{\theta}_s - K_j \theta_s + K_j \theta_m}{J_s} \end{array} \right\}$$

One more parameter should not be missed, which is the temperature of the actuator specially the part that concern the winding. regard to the instruction, the temperature of the inner winding must not overpass $T_{wmax} = 125°C$, traslating this fact into electric circuit illustrated in Figure 5.2.

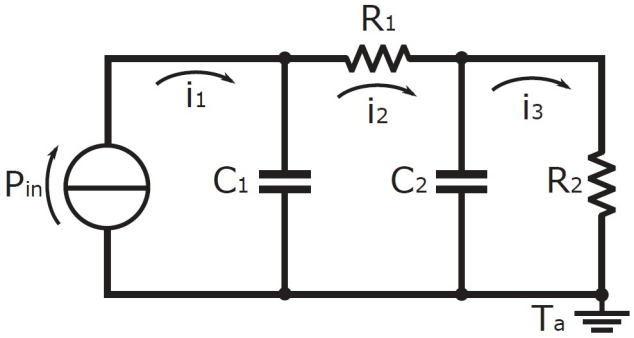

Figure 5.2: Equivalent electric model for thermal calculations. [5].

checking the source of heating we can define the dissipated power in this equation $P_{in} = Ri^2$ and regard to the equivalent circuit it's equal to the current i_1 as in previous depicted. from the data sheet represent both the capacitance and thermal resistance both are caring the heat exchange from the inner winding to its cover and from its cover to ambient. in the flowing equation we are able to calculate the capacitance $C = \tau/R$ knowing the τ thermal time constant as shown in the next table. Regard to the above Equivalent electric model, the voltage that we acquire from the resistor it is equal to the temperature of the winding's ($T_1 = V_1$) and of it's cover ($T_2 = V_2$), concerning these calculation the Laplace transform model will be:

$$\left\{ \begin{array}{c} i_1 = P_{in} \\ \frac{1}{sC_1}(i_2 - i_1) + R_1 i_2 + \frac{1}{sC_2}(i_2 - i_3) = 0 \\ \frac{1}{sC_2}(i_3 - i_2) + R_2 i_3 = 0 \end{array} \right\}$$

Description	Symbol	Value
Nominal voltage	V	$24\,\mathrm{V}$
Terminal resistance phase to phase	R	$1.39\,\Omega$
Terminal inductance phase to phase	L	$2.26 \times 10^{-4}\,\mathrm{H}$
Speed constant	K_v	$465\,\mathrm{rpm/V}$
Torque constant	K_m	$0.02\,\mathrm{N\,m\,A^{-1}}$
Motor viscous friction	c_m	$5.54 \times 10^{-5}\,\mathrm{N\,m\,s\,rad^{-1}}$
Motor inertia	J_m	$2 \times 10^{-6}\,\mathrm{kg\,m^2}$
Joint stiffness	K_j	$16\,\mathrm{N\,m\,rad^{-1}}$
Spool inertia	J_s	$1.18 \times 10^{-9}\,\mathrm{kg\,m^2}$
Spool viscous friction[1]	c_s	$8.166 \times 10^{-4}\,\mathrm{N\,m\,s\,rad^{-1}}$
Thermal parameters		
Thermal resistance windings-housing	R_1	$5.4\,\mathrm{K\,W^{-1}}$
Thermal resistance housing-ambient	R_2	$2.5\,\mathrm{K\,W^{-1}}$
Thermal capacitance windings-housing	C_1	$5.4\,\mathrm{J\,K^{-1}}$
Thermal capacitance housing-ambient	C_2	$5.4\,\mathrm{J\,K^{-1}}$
Ambient temperature	T_a	$25\,^{\circ}\mathrm{C}$

Figure 5.3: Data for electromechanical and thermal systems simulation [5].

when the heat transition we know the value of i_2 and i_3, the cover's and winding's temperatures can be detected following this approach :

$$\left\{ \begin{array}{c} T_2 = T_a + R_2 i_3 \\ T_1 = T_a + R_2 i_3 + R_1 i_2 \leq 125^{\circ} \end{array} \right\}$$

after all these concerning we are ready to execute the whole model through Simulink as illustrated in Figure 5.4.

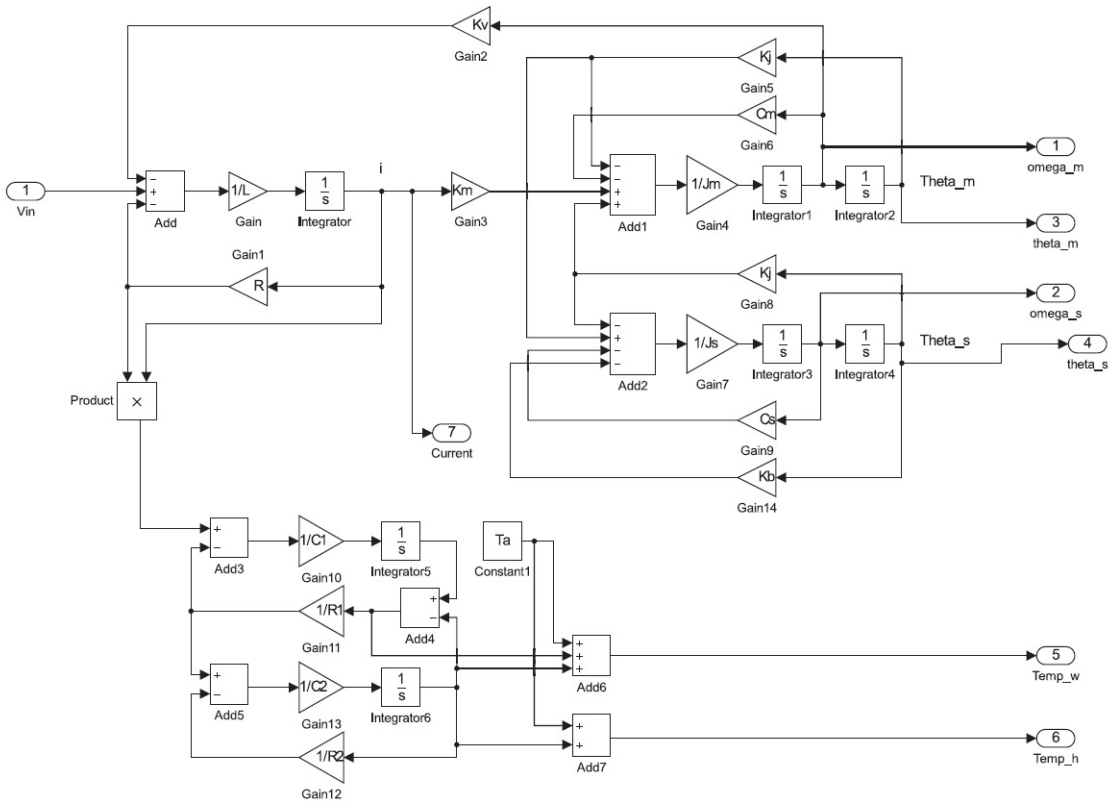

Figure 5.4: Model implementation in the Simulink software [5].

5.2 Spool Torque Control

The motor must generate proper torque taking in account some consideration, in order to calculate the proper torque we need to implement our dynamic model into transfer function by derive equation of motion and other equations. starting with dynamic shear viscosity of a fluid expresses its resistance to shearing flows(as shown in figure 5).

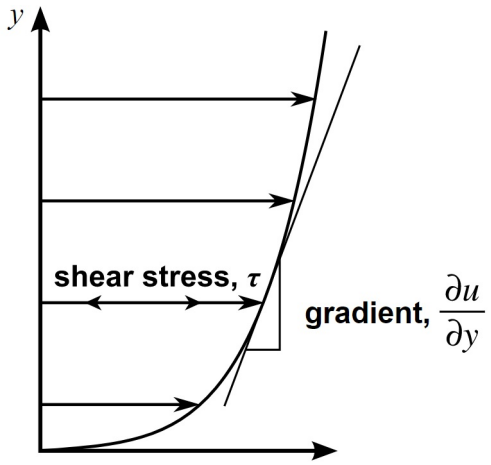

Figure 5.5: parallel flow between spool and the sleeve , the shear stress is proportional to the gradient of the velocity.

and it represents in Equation 5.3, where($\mu = 0.01pa*s$) is a dynamic viscosity of the fluid and it is proportionality factor, A it cover the area that contact the spool and and the fluid $A = 2\pi rL$, $(L = 34.5 * 10^{-3}m, r = 7.7 * 10^{-3}m)$, and U is the fluid velocity and h is altitude between the spool and the sleeve $(h = 0.015 * 10^{-3}m)$.

$$F = \mu A \frac{U}{h} \tag{5.3}$$

then, moving to the relation between linear and angular velocity $v = r\Omega$ coupled with force and toque relation we get this Equation5.4.

$$T = \frac{\mu r^3}{h} A\Omega \tag{5.4}$$

expanding the area A and replace it in the equation, and combine the constant values into letter C ($C = 6.597e - 05$) as can you see in Equation 5.5 and Equation 5.6.

$$T = \frac{\mu r^3}{h} 2\pi L\Omega \tag{5.5}$$

$$T = C\Omega \tag{5.6}$$

returning to the main Equation that represent the total Torque applied on the spool (as can you the Equation 5.7).

$$T_{tot} = T_0 + T_\Omega \tag{5.7}$$

$$T_{tot} = J\dot{\Omega} + C\Omega \tag{5.8}$$

In Equation 5.8) J represent the second moment of inertia of the spool ($J = 1343.3 * 10^{-9}$), now the equation ready to transform it into transfer function as can you see in the Equations Equation 5.9)

$$\frac{\Omega}{T_{tot}} = \frac{1}{sJ + C} \tag{5.9}$$

$$\frac{\Theta}{T_{tot}} = \frac{1}{s^2 J + Cs}$$

$$\frac{\Theta}{T_{tot}} = \frac{1}{s(sJ + C)} = \frac{1}{s} * \frac{1}{sJ + C}$$

$$\frac{\Theta}{T_{tot}} = \frac{1}{s} * \frac{1}{sJ(1 + \frac{C}{sJ})} = \frac{1}{s} * \frac{\frac{1}{s}\frac{1}{J}}{1 + C\frac{1}{s}\frac{1}{J}}$$

Now the model is ready to convert it into function block and test it on simulink, the aim to try different values of T_{tot} to get the proper angle ($\Theta = 22.5°$) (as can you see in Figure 5.6).

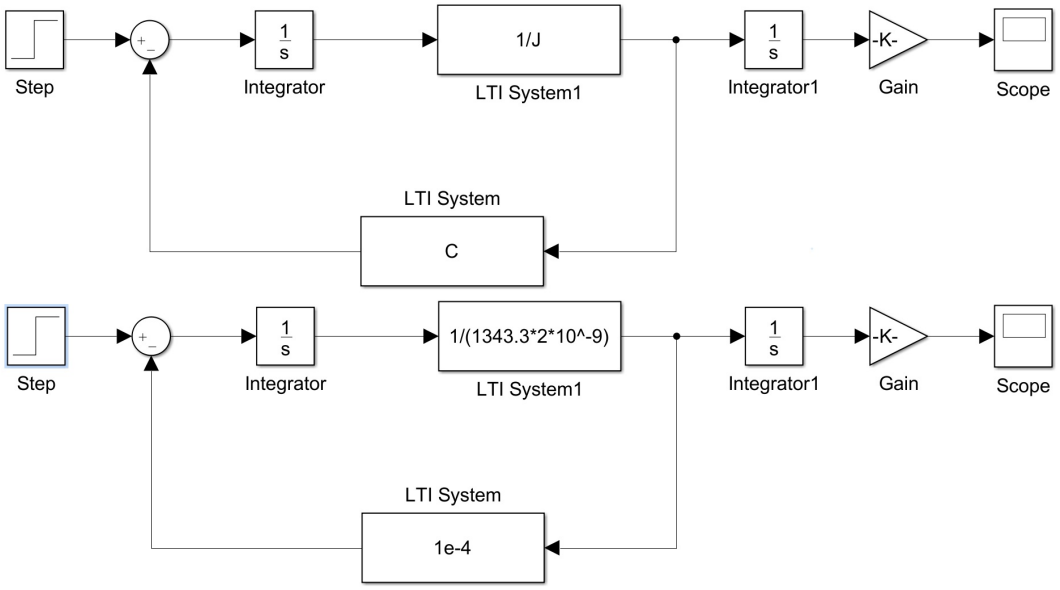

Figure 5.6: Function block diagram to derive T_{tot} (system 1).

before we move to the final result, we took in account some consideration as we can see in the last Figure 5.6). Firstly we multiply the value J by 2 because we assume also the moment of inertia of the magnet part. Secondly, we change the value of the constant C into $1e{-}4$ because we assume also the safety factor Thirdly, we add a spring bar (Failure mechanism) act against the

motor rotation we will describe that later in chapter 8, this bar has a stiffness ($k = 0.0606[\frac{N*m}{rad}]$), it has placed in function block to have full view as we can see in Figure 5.7

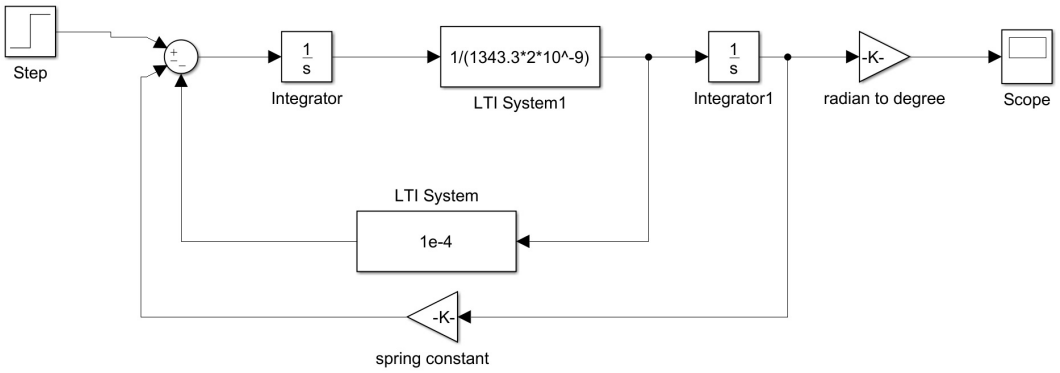

Figure 5.7: Function block diagram to whole system including spring bar.

Our interest to find the proper torque after 10 ms,the estimated torque is 0.02867 Nm, it is the torque that required to rotate the spool and twist the spring bar 22.5° as you can see in Figure 5.8

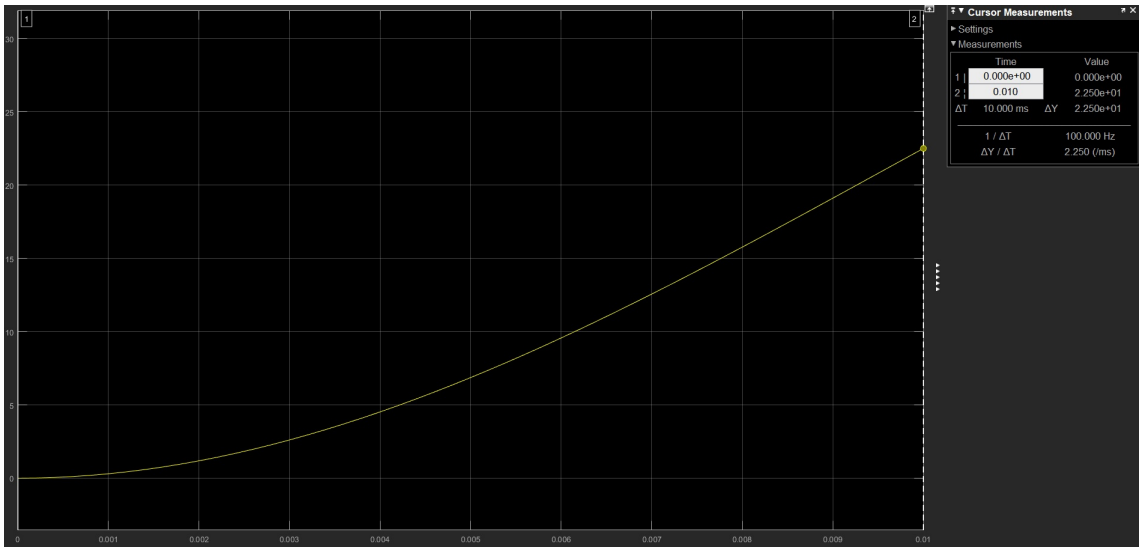

Figure 5.8: the scope shows that amount of torque reach the exact degree that we aimed.

5.3 Valve Torque Observation

During our studies we have noticed that the torque which acts on the walls of the spool inside the valve is not fixed, there is different amount of torque acts inside of the valve every time we change the pressure drop and aperture angle, to clarify this idea we made a map of the velocity vectors that acts on the spool walls inside the valve as you can see in this Figure5.9.

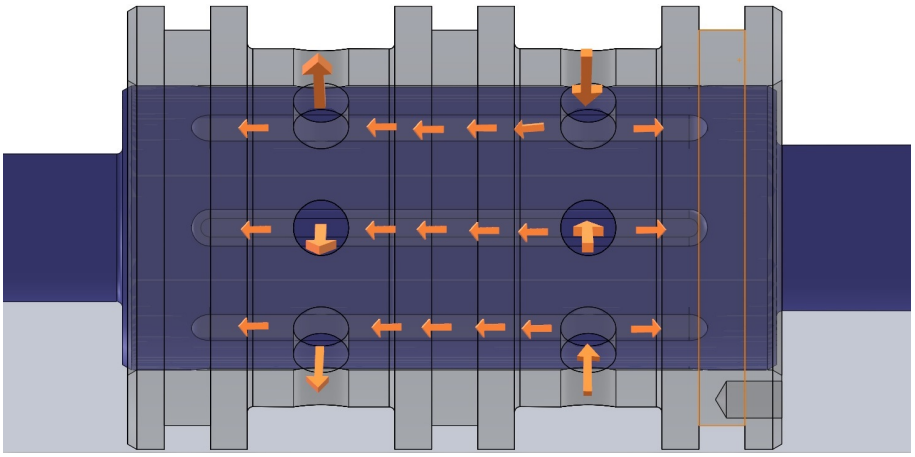

Figure 5.9: side view for the velocity map of the spool and the sleeve.

As you can this Figure the velocity vectors go through the sleeve and move on between the channels and go out through the sleeve as well. In the Figure5.10 you would see the isometric and the cross section depiction of the outlet port, in (fig 5.10(a)(b)) the flow of the fluid goes directly from the spool to outlet port through the sleeve without performing any force on the spool walls, in (fig 5.10(e)(f)) we face the same issue that there is no force act on the spool walls, but in (fig 5.10(c)) and specially in (d) depiction where the valve partially open, we can see how the fluid increase his velocity specially at the point between the spool and the output port, so the fluid particularly perform force on the spool walls and increase amount of torque that act on the spool comparing with first two cases.

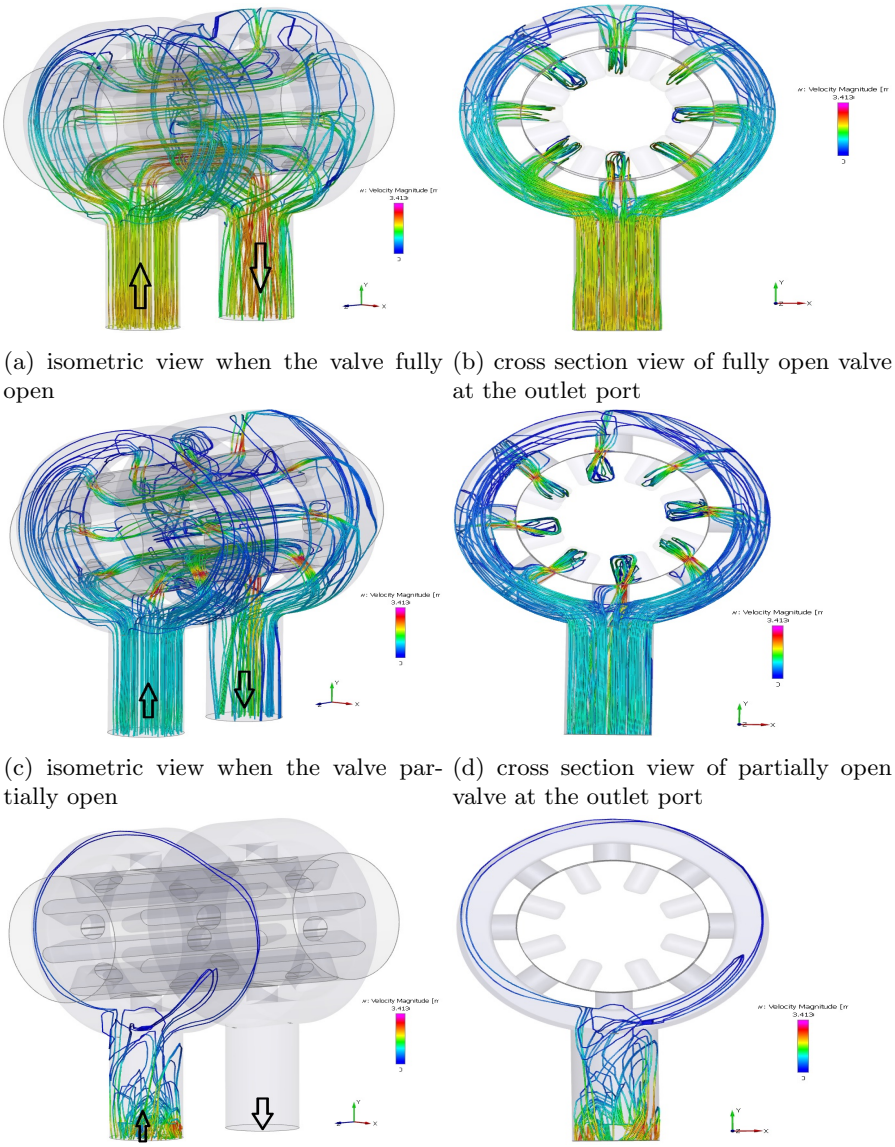

(a) isometric view when the valve fully open

(b) cross section view of fully open valve at the outlet port

(c) isometric view when the valve partially open

(d) cross section view of partially open valve at the outlet port

(e) isometric view when the valve fully close

(f) cross section view of fully close valve at the outlet port

Figure 5.10: velocity map of the fluid inside the valve

This observation lead us to recalculate the torque that act on the valve at different aperture angle and different pressure drop , and the result would be plot in the Figure5.11, as it shown in the plot, the torque at the small or high aperture angle(mean where the is valve fully close or fully open) the toque is very small , almost negligible comparing when the valve is half-way open, so the

most critical condition is when the valve is half-way open.

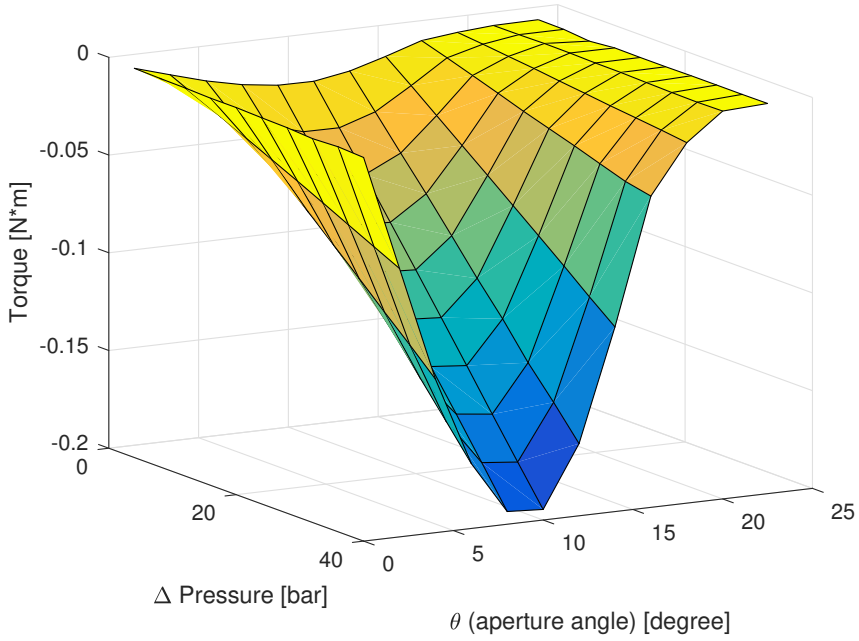

Figure 5.11: side view for the velocity map of the spool and the sleeve.

5.4 Motor length estimation

The simulation was set up in the LIM labortary, the device was simulated using COMSOL Multiphysics as you can see in Figure5.12 is the cross section of the motor and the spool.

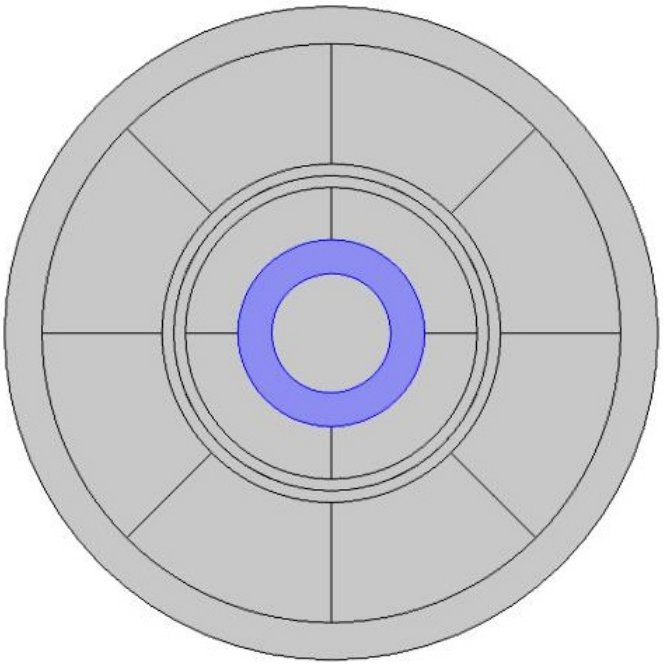

Figure 5.12: cross section of the model, the area in blue represent the spool and the blocks near of it represent the permanent magnets, the other blocks represent the winding of the motor.

The torque that show in the software is the torque density, so the torque can be controlled by modify the length of the motor because the torque is proportional to the length. the length of the motor is around 26 mm , that is the required length to produce required torque.

Chapter 6

Design tools for the prototype

To do a design is either work out a project for some requirements or to fix a particular problem. The aim of the design is to create a real physical object , at that point the item should be useful, protected, dependable, usable, aggressive , industriable[4].

6.1 Design Considerations

Some of the time the quality expected of a component in a framework is a critical factor in the assurance of the geometry and the dimension of the component. In such a circumstance we may say that the strength is one many important properties we should take in account, when we refer to this properties it may affect the hole system. Generally a significant number of such attributes must be considered and organized in a given plan circumstance. Many of the important components are illustrated in Table 6.1 [3].

Some of these characteristics have to do with the dimensions, the material, the handling, and the joining of the components of the framework. many features could be interrelated, which influences the arrangement of the hole system.

6.2 Design spring bar

The most important point for a designer is to check the ultimate tensile strength and compare it with the maximum stress at the specific points, it should be lower than the maximum tensile stress. These procedure is necessary to guarantee the safety for any design parts. Stress is a state property at a particular point inside a body, which is a component of stack, geometry, temperature, and assembling preparing. The aim of the safety bar to return the spool to the previous state, the bar would be fit in the prototype as shown the green bar in Figure 6.1, from

Table 6.1: characteristics must be considered for a design [1]

1 Functionality	14 Noise
2 Strength/stress	15 Styling
3 Deflection/stiffness	16 Shape
4 Wear	17 Size
5 Corrosion	18 Control
6 Safety	19 Thermal properties
7 Reliability	20 Surface
8 Manufacturability	21 Lubrication
9Utility	22 Marketability
10 Cost	23 Maintenance
11 Friction	24 Volume
12 Weight	25 Liability
13 Life	26 resource recovery

one side it hinged by the spool and from other side it hinged by grub screw. The function is when the motor rotate the spool to open the valve, it rotate and twist the bar as well,after turning off the motor the bar will rotate the spool to the initial state where the valve is closed.

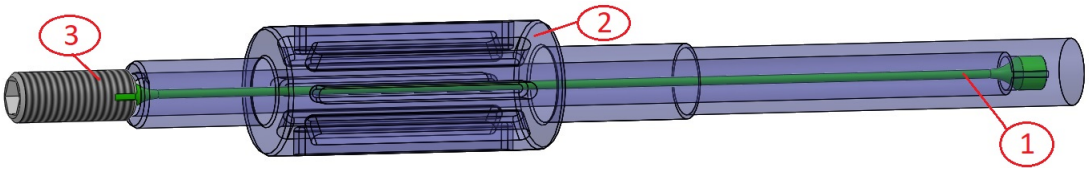

Figure 6.1: ① Saftey bat, ② spool, ③ Grub screw with carving .

The selection of a material for a machine part or a structural member is one of the most important decisions the designer is called on to make. The decision is usually made before the dimensions of the part are established. For this bar we chose the material Alloy Steel A36, which has characteristic such as Yield strength equal 250 MPa and Ultimate strength equal to 400 MPa. There are methods for estimating stresses and deflections of machine members are presented. These estimates are based on the properties of the material from which the member will be made. After choosing the material we designed the bar with these figures(the inner diameter is 1mm, the outer diameter is 5mm, the length is 120mm). By calculating the K (rotational stiffness) we are able to assume the required torque to twist the bar 22.5° as shown in Equation 6.1 :

$$K = \frac{M}{\theta} = \frac{0.0238}{0.392699} = 0.0606 \left[\frac{N * m}{rad}\right] \tag{6.1}$$

The rotational stiffness was implemented in the Function block diagram as

we mentioned previous in Figure 5.7, then we extract this value $0.02379N * m$ (the required torque that act on the spring bar). In the SolidWorks simulation we examined the bar by acting the exact torque and test the elasticity as you can see in Figure 6.2.

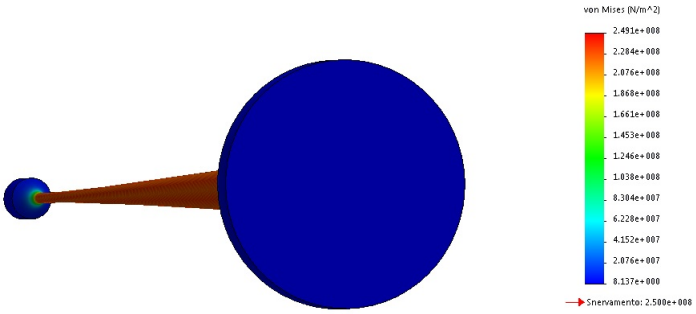

Figure 6.2: Elasticity simulation for the spring bar .

Follow the von Mises criteria we found the maximum stress that act on the bar is $2.491e^8$[pascal] and it is less than Yeild strength, so we can be sure that the bar would stay in elastic state.

6.3 Design Bearing

The main idea of lubrication is to maintain the distance between the intended parts also to reduce the heating caused of relative motion of the mechanical component. we can see these types of bearing at many cases like a shaft in a sleeve , bushing, or any relative motion sliding or rolling. The combination of designing and the science of material knowledge, allow us to satisfy the requirements to produce the best component with very good reliability. The aim of this section is to design a bearing for the rotating spool in the mainfold as you can see in Figure 6.3.

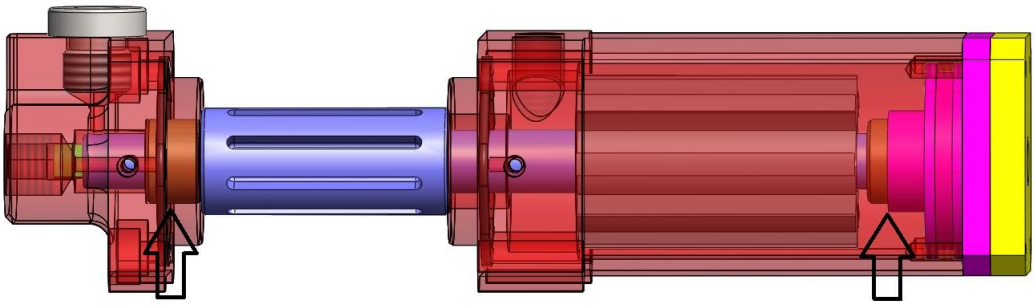

Figure 6.3: two bearing for the spool placed at the indicating arrows .

the inner dimension its 8mm and the outer dimension its 12mm ,the drag coefficient has calculated previously in chapter 7. Hydro-static lubrication has chosen as a type of lubrication, it works at the load-bearing area where the pressure is high enough it separate the surfaces with a relatively thick film of lubricant.

Chapter 7

Future work

Since the studies has started in 2015, the team of LIM (Laboratorio Interdisciplinare di Meccatronica) has been developing this model to achieve the goals that match the requirements and improve the functionality of the prototype, moreover, the model is still under expansion there are many development is still to be made. One of these improvements is to repeat the first experimental evaluation like the one in Experimental damping characteristic developed by the valve assembly for different opening percentages as shown in Figure 4.6 trying to be more accurate evaluating the the pressure drop and at the same time repeat some simulations on the PumpLinx software to match the exact characteristics of the curves, by this repetitions we are able to obtain the precise difference of their features. secondly, do the experimental part after these researches, study and observe the the results, Moreover, add the designed parts (the spring bar and the bearing) to the model, first of all we need to manufacture these parts at first place as they designed. Then we can apply the torque that we have calculated on the spool as shown in chapter 7 , and observe the rotation of the spool regards to the aperture angle, matching the results of the simulation and the experimental parts. Testing of theory is required to validate methods of analysis and to give confidence in theory for design work. This is likely to involve testing of individual parts, of complete valves in a steady-flow circuit , or testing of complete dampers to relate damper characteristics to valve characteristics, to investigate piston or rod seal friction effects, etc. Performance testing is required to check that prototypes or samples of production dampers meet their specifications within tolerance, and are adequately consistent one to another. In competition, performance testing is required to check that a given valve set-up gives the expected behaviour.

Chapter 8

Summary

The aim of this thesis is to develop an electrohydraulic shock absorber act like a variable damper, this object achieved by checking the flow of the fluid through the spool valve and adjusting the pressure drop and the aperture angle of the spool in order to regulate the damping force.

In Politecnico di torino,the Mechatronics laboratory has started up working on (semi-active shock absorber based on a rotary spool valve) trying to study the features and improve the functioning of the damper, as a matter of fact This studies has started a couple of years ago in LIM (Laboratorio Interdisciplinare di Meccatronica) at Politecnico di Torino collaborate with MESAP.

The prototype consist of many components, starting with the damper housing and it works like a passive damper, the manifold it links the house from upper side , it contains the most interesting parts like the spool and the sleeve in which the valve can be controlled, the inlet plugs those are hosted in the manifold, the brush-less EC engine the one that control the spool inside the valve through elastic joint, the safety bar the one which return the valve into initial state, the bearing and the drain system which there are also parts of the prototype.

The principle thought is that the valve goes into two states , open and close. When the valve open, the valve permit the fluid flow through the system, in this action we reduce the damping characteristic, but if the valve is closed the system would work like a passive damper and also we will have a high damping condition. we can control the damping force specially with this kind of valves. In this model we can control the range for damping characteristic and we can control the required force, this can be achieved by controlling the position of the spool by EC motor.

Initial studies were used COMSOL Multiphysics software platform for modelling and simulation the functioning of the valve. In this thesis we used

PumpLinx®, it is a Computational Fluid Dynamics (CFD) tool, advance software which can provides accurate virtual testing for the analysis and performance prediction of fluid for many mechanical components including our prototype. Where have implemented the prototype in the software and provided some simulations. Before start the simulation the model should pass three different preparation when the prototype has been implemented, the surface preparation, mesh preparation, model preparation. The simulation has been studied for the valve at different stages and different states, firstly the simulation was applied for a set delta pressure from 4 bar to 40 bar with linesapce equal 4, I mean like (4, 8, 12, 16, ...40), in order to cover all probable pressure the valve system could face, also the simulation was applied for a different aperture angle for the valve, form 0 degree to 22.5 degree with linespace equal to 2 degree (2, 4, 6, ...22.5), notice that changing the angle from 0 to 22.5 it is enough to close or open the valve. The simulation was made to measure the volumetric flow rate at the outlet port at those stages that we mentioned before. From the results we can analyze many things, firstly , the volumetric flow goes spontaneously every time we change the any parameter, for example at a fix aperture angle , every time we increase the delta P the volumetric tense to increase, on second hand, Every time we increase the aperture angle (turn to close the valve) the volumetric turn to decrease. However, these studies can provide us the measurement of the simulation, which can tell us that the fluid goes spontaneously and we get reasonable results.

Results comparison (experimental - simulation). The aim of this comparison is to calculate the difference (error) between experimental and simulation results by obtaining the experimental flow rate (Qexp) from the exponential curves in the measured points, and interpolate the results from the simulation that matches both aperture angle and delta pressure. Refer to the result that we have from the Tables we can realize the error is a little bit height at the small aperture angle, the cause of these height error refer to inaccurate observation during the experimental tests, but at the same time we can see at the high aperture we have almost matched results as we can see from Table.

The motor must generate proper torque taking in account some consideration, in order to calculate the proper torque we need to implement our dynamic model into transfer function by derive equation of motion and other equations. starting with dynamic shear viscosity of a fluid expresses its resistance to shearing flows. Our interest to find the proper torque after 10 ms,the estimated torque is 0.02867 Nm, it is the torque that required to rotate the spool and twist the spring bar 22:5 degree.

Valve Torque Observation. During our studies we have noticed that the torque which acts on the walls of the spool inside the valve is not fixed, there is different amount of torque acts inside of the valve every time we change the pressure drop and aperture angle, to clarify this idea we made a map of the velocity vectors that acts on the spool walls inside the valve, This observation

lead us to recalculate the torque that act on the valve at different aperture angle and different pressure drop , so the result shows that the torque is negligible at the small or high aperture angle(mean where the is valve fully close or fully open), it is small comparing when the valve is half-way open, so the most critical condition is when the valve is half-way open.

Motor length estimation, the device was simulated using COMSOL Multiphysics, The torque that show in the software is the torque density, so the torque can be controlled by modify the length of the motor because the torque is proportional to the length. the length of the motor is around 26 mm , that is the required length to produce required torque.

Design spring bar (safety bar), the would return the spool to the initial state after the motor turn off, the design consist of two part, first to choose the material which it is alloy steel A36 , second to some torsion test on the bar to ensure that the bar would not fracture, after analytically calculation and software simulation of torsion test we found the best design of the bar 120mm long the inner diameter 1 mm and the outer diameter 5 mm, Follow the von Mises criteria we found the maximum stress that act on the bar is 2.491e8[pascal] and it is less than Yeild strength, so we can be sure that the bar would stay in elastic state.

Bibliography

[1] Richard Gordon Budynas, J Keith Nisbett, et al. *Shigley's mechanical engineering design*, volume 9. McGraw-Hill New York, 2008.

[2] Avesta Goodarzi and Amir Khajepour. Vehicle suspension system technology and design. *Synthesis Lectures on Mechanical Engineering*, 1(1):i–77, 2017.

[3] Honghai Liu, Huijin Gao, and Ping Li. *Handbook of vehicle suspension control systems*. Institution of Engineering and Technology, 2013.

[4] Sergio M Savaresi, Charles Poussot-Vassal, Cristiano Spelta, Olivier Sename, and Luc Dugard. *Semi-active suspension control design for vehicles*. Elsevier, 2010.

[5] Andrea Vellante. Semi-active shock absorber based on a rotary spool valve. *modelling shock absorber*, 1(1):93–102, 2015.